RIJKSWATERSTAAT COMMUNICATIONS

Nr 11

THE HARINGVLIET SLUICES

by

Ir. H. A. Ferguson
Ir. P. Blokland
Ir. drs. H. Kuiper

1970

Directoraat-Generaal Rijkswaterstaat
Informatie en Documentatie
Postbus 20906
2500 EX Den Haag
Tel. 070-3518004 / Fax. 070-3518003

RIJKSWATERSTAAT COMMUNICATIONS

THE HARINGVLIET SLUICES

by

Ir. H. A. Ferguson, Deltadienst

Ir. P. Blokland, Directie Sluizen en Stuwen

Ir. drs. H. Kuiper, Directie Bruggen

1970

Any correspondence should be addressed to

DIRECTIE ALGEMENE DIENST VAN DE RIJKSWATERSTAAT

THE HAGUE — NETHERLANDS

The views in this article are the authors' own.
Section I by Ir. H. A. Ferguson
Section II by Ir. P. Blokland
Section III by Ir. drs. H. Kuiper

Contents

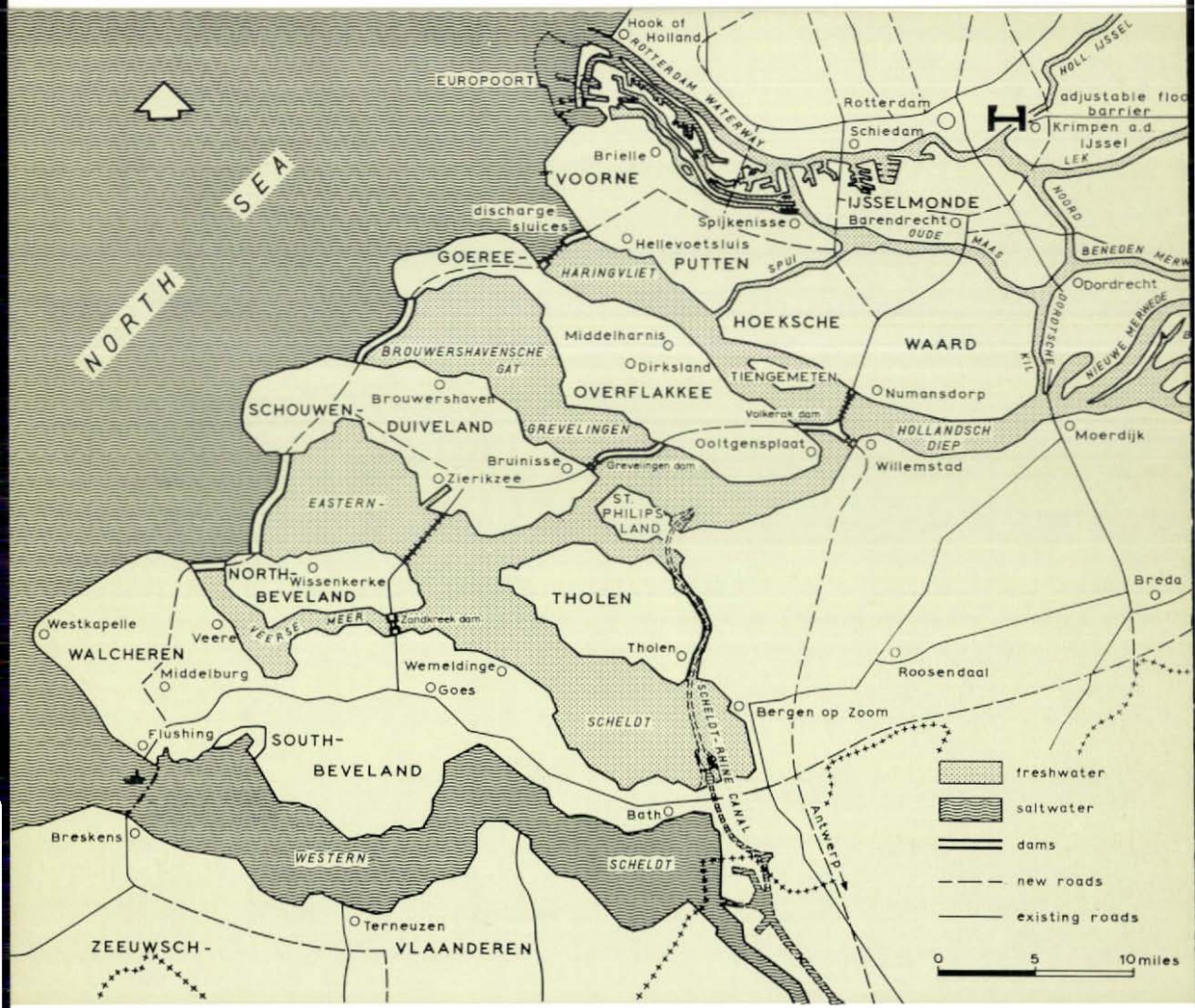

Figure 1. The Delta Plan

I. The sluice-gate complex

1. Location and purpose of the Haringvliet sluices in the Delta area

The main purpose of the Delta Project is to protect the low-lying Rhine-Meuse delta in the south-western part of the Netherlands more effectively against very high tides; the disastrous storm tide in 1953 showed only too clearly how vulnerable this area was because of its structure, allowing the sea to penetrate far into the country through a number of broad and deep inlets. Broadly, the scheme consists in damming up the three large estuaries between the Western Scheldt in the south and the Rotterdam Waterway in the north, both of which will have to remain open to shipping (Figure 1). In addition to the three main closures, i.e. of the Haringvliet, the Brouwershavensche Gat and the Eastern Scheldt, the scheme includes the building of several secondary or auxiliary dams, viz. the Zandkreek dam, the Grevelingen dam and the Volkerak dam. These auxiliary dams are necessary to counter the danger of freak tidal currents running in the various estuaries that would otherwise be induced in the periods between the successive closures of each estuary. The Volkerak dam also separates the northern from the southern part of the delta, so that their water economies need not be identical. In the matter of water economy, the function of the new inland lakes to be formed in the area south of the Volkerak dam may to some extent be compared to that which Lake Yssel will have in the north; they will likewise constitute important fresh-water reservoirs.

The Delta waters north of the Volkerak dam will continue to be in open communication with the sea through the Rotterdam Waterway, so the area will still be tidal, although the tidal movements will be greatly moderated. The waters from the Rhine and Meuse will also continue to flow to the sea through this area. Formerly the water coming down these rivers could reach the sea along three different routes, viz. through the Rotterdam Waterway, the Haringvliet and the Volkerak. The dams across the Volkerak and the Haringvliet will bar the latter two escape routes, so if no other measures were taken all the water would have to pass through the Rotterdam Waterway. This sets no problem when the discharge of the rivers is small, but this waterway alone would not be able to cope with fairly large quantities. Consequently, at least one more outlet to the sea must be provided. This is why a row of sluice gates has been incorporated in the Haringvliet dam of great enough capacity when they are wide open to handle, together with the Rotterdam Waterway, the largest conceivable river-water discharge during ebb tides.

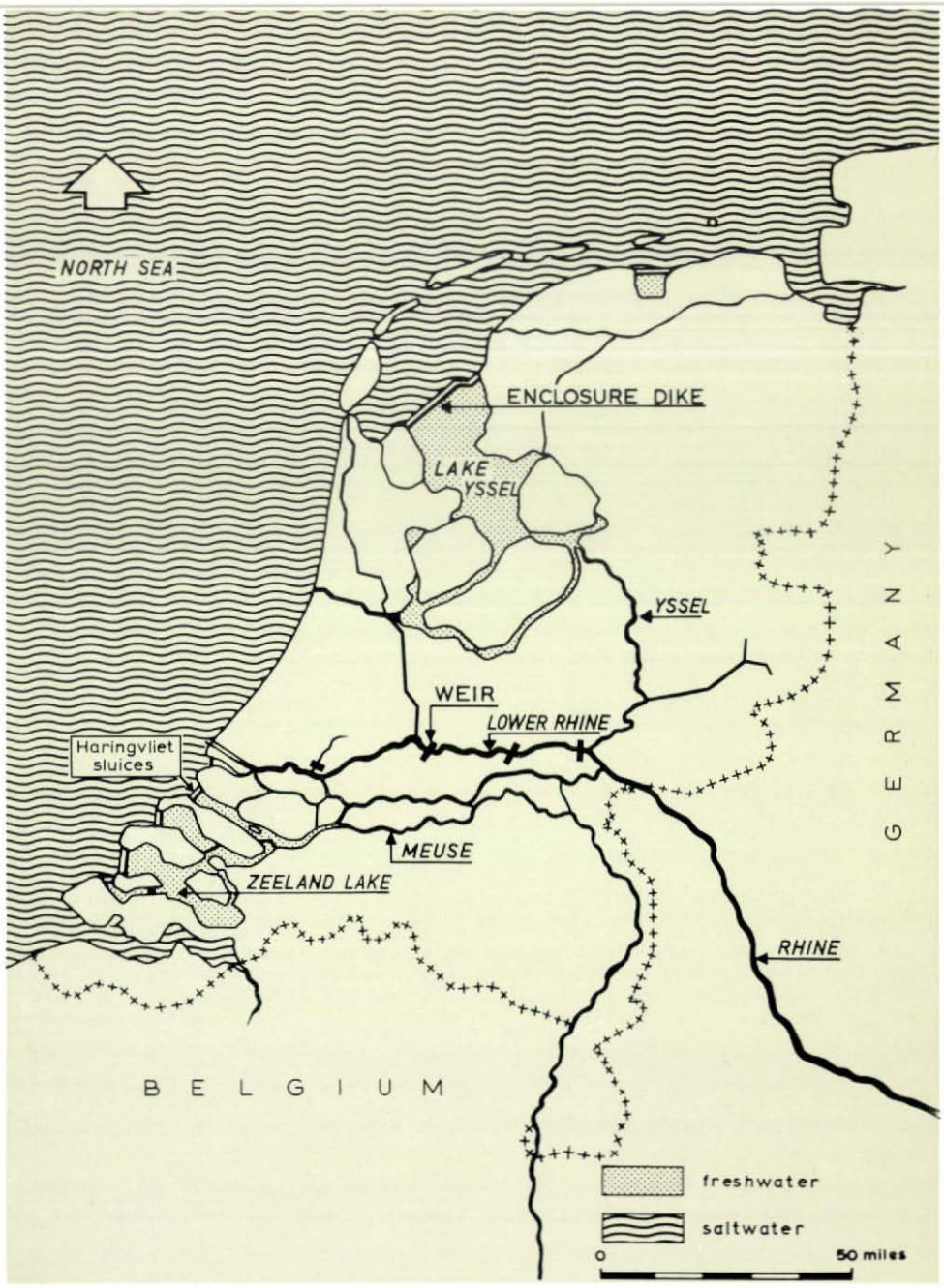

Figure 2. The freshwater basins in the Netherlands

The sluice gates will remain closed at high tide so as to provide the greatest possible protection against flooding and salt penetration. When the river discharge is normal, the gates will only be partially opened at low tide to maintain the largest possible discharge through the Rotterdam Waterway compared with that before the damming off of the estuaries. The greater volume of fresh water passing through the Rotterdam Waterway will improve the water economy, since salt penetration along this route, which is considerable in this deep shipping channel, is suppressed by the larger outflows. In view of this, the Haringvliet sluice gates will help us to bring about an optimum distribution of outflowing river water over the two routes, viz. the Haringvliet and the Rotterdam Waterway.

So, in addition to providing protection against storm tides the Haringvliet sluices will also provide the best possible means of pushing back the salt-penetration limit within the capacity of the system of gullies, which is of course restricted in view of the current velocities permissible in connection with shipping and erosion. To distribute the outflows of river water in the desired manner, the sluice gates will have to be operated in conjunction with the regulation of the discharge down the Rhine between Arnhem and Rotterdam; this has been made possible by placing three weirs in this river by means of which the quantities of water flowing into Lake Yssel can be controlled (Figure 2). Consequently, the Haringvliet sluices are not only part of the Delta Project but are also a very important part of the national system of sluices and weirs which make it possible for Holland's water economy to be managed advantageously by artificial means.

The Haringvliet system of sluices is therefore not only a storm tide barrier, playing its most important part with its gates closed to withstand the force of the sea, but also an instrument by which the discharge of water can be regulated at will. Consequently, the gates must not only be sufficiently strong but also easy to operate; the entire mechanism has been very carefully designed indeed to ensure ease of adjustment and operation.

Than there is a third important requirement the sluice-gate complex must meet. In severe winters ice floes, which make their appearance after the thaw has set in, must be able to reach the sea. A certain proportion will therefore have to pass through the sluice gates, so the openings must be wide enough to take ice floes and provisions have had to be made for ice breakers to operate inside and in front of the sluice gates to ease the passage of ice.

The space between the piers could not be calculated exactly; in the light of past experience in Dutch rivers it was thought that the gaps would have to be at least 50 metres wide to make sure that with the aid of ice breakers large floes could pass between the piers without getting jammed. The openings were made as wide as was

Photograph 1. View of the closed Volkerak on the upper half of the picture running from left to right with the Volkerak dam (photo Bart Hofmeester)

considered acceptable in view of their design; the width between piers is 56.5 metres. The depth of the sill of the gates was partly determined by the need for ice breakers to pass through them at low tide; it was fixed at 5.5 metres below Amsterdam Ordnance Datum (A.O.D.).

The sluice complex has 17 openings and its overall width is over 1,000 metres; it has an effective total aperture of about 6,000 sq. metres at half tide.

2. Hydraulic boundary conditions adopted for project

Another important boundary condition was set by the wave attack which the structure would have to withstand in extreme conditions, when the sea may be swept up to 5 m above A.O.D. The shape of the seaward gate is not the best for withstanding wave attack; a vertically placed gate would undoubtedly have been subjected to a much smaller wave load. But the desire not to subject the hoisting mechanism operating the gates to too great a strain called for a compromise. Because of their segmented shape the resultant of the forces now runs through the centre of rotation of the gates, so when they are lifted the resistance is far less than it would have been if straight gates had been installed. The need to keep the power absorbed by the hoisting mechanism within reasonable limits was the deciding factor.

Before the stresses to which the gates might be subjected by wave attack could be determined, as much information as possible had to be obtained on the wave motion that might be expected in front of the sluices under extreme conditions. It was not enough to determine the significant height of the waves at that spot; as much information as possible had also to be obtained on the wave spectrum and the shape of the wave crests. Wave observations made from lightships in the North Sea were very useful, though they only provided information on wave heights. Recordings of wave movements (height and periodicity) transmitted by a number of wave-measuring "poles" off the coast and inside the estuary were used, together with what is called the energy spectrum. The manner in which the wave motion at sea thus approximated would be transmitted to the sluice-gate complex was then studied. Refraction calculations were prepared for the purpose and supplemented with radar observations of the original wave pattern in the estuary (Figure 3).

It was also necessary to conduct an extensive model test in a wind flume (Figure 4).

The model test revealed that the wave stresses consisted of sharp high-pressure peaks which would subject the structure to impact stresses (Ref. 1). These peaks could cause the whole structure to vibrate; but vibration of this nature has been taken care of by adopting a high impact coefficient when calculating the dimensions of the structure. The peak value of the wave impact (Ref. 1 and 2) has been reduced considerably by making fairly substantial alterations to the cross section of the original

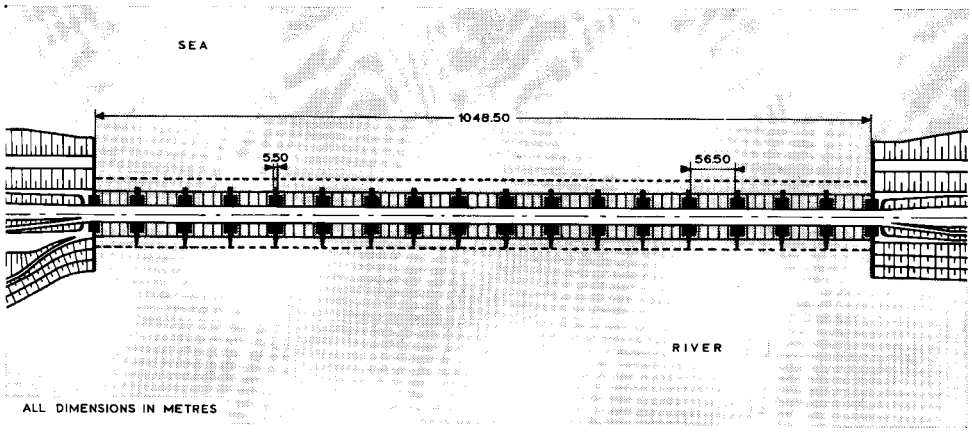

Figure 3a. Plan of the sluices complex

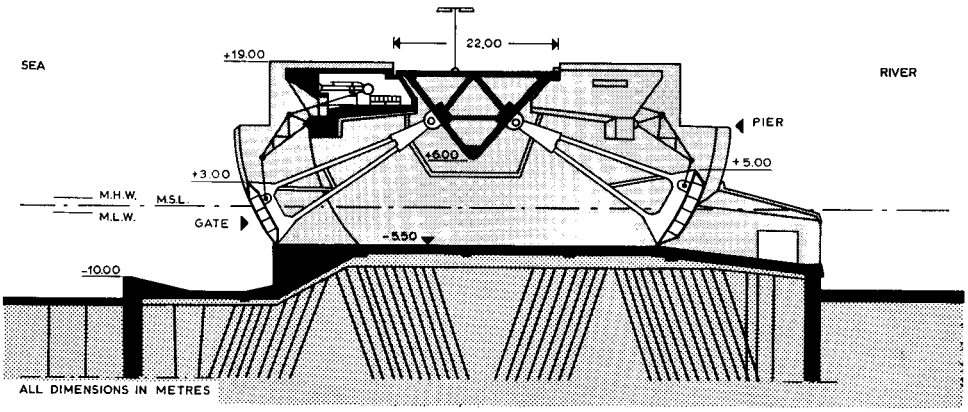

Figure 3b. Cross-section of the sluices complex

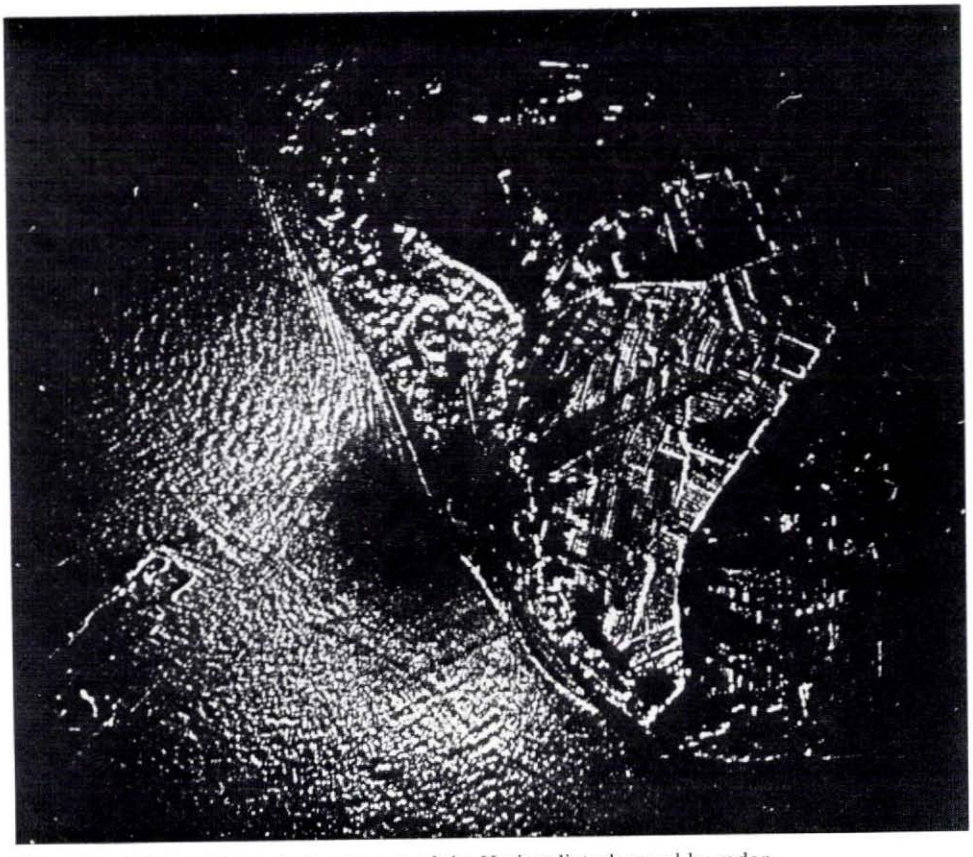

Figure 3c. Wave patterns in the estuary of the Haringvliet observed by radar

design. It was impossible to eliminate the pressure peaks altogether. The occurrence of pressure peaks in wave attack was seen to be determined largely by the shape of both the waves and the gates. During a storm in the prototype the waves may be expected to have fairly steep crests and in order to reproduce this steepness in the model, the waves in it were also virtually generated by wind only. Accordingly, the waves in model will show wide variations in height more or less corresponding to the prototype and consequently in steepness. As a result, the peak wave stresses also varied widely in magnitude in a test (Ref. 3). However, since circumstances may vary also widely in the prototype, both during a single storm and during several storms, a statistically oriented approach to the evaluation of the results of the model test was essential.

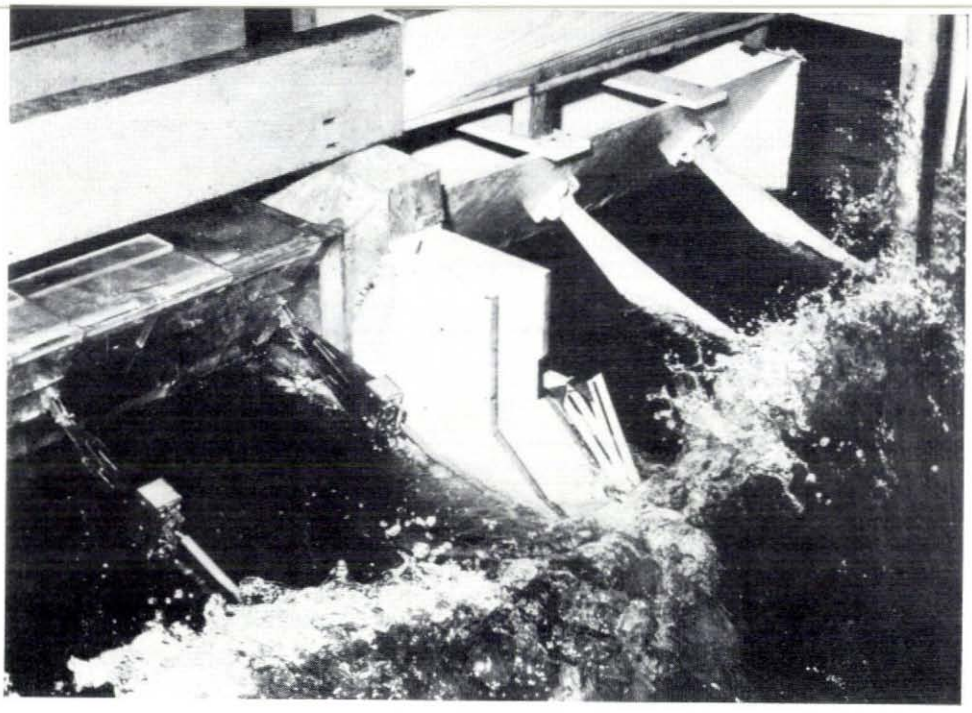

Figure 4. Wave attacks on the sluice gates in the model tests in a wind flume of the Hydraulics Laboratory

The wave observations at sea also had to be reproduced in statistical form. These observations were studied together with the results of the model test and a frequency curve was obtained of the wave stresses that may be set up while the gate is operational. The latter stress was taken as the basis for the design calculations; the likelihood of its being exceeded is 10^{-4} per year (Ref. 4).

As already stated, the shape of the seaward gates is not the best to withstand wave attack. Consequently, they will be subject to very heavy buffeting. The landward gates are in a much more favourable position vis-à-vis the waves rolling in from the sea. The inner gates would therefore better be able to withstand wave attack from the sea if it were not for the fact that the points of support are subjected to tension, a drawback that partly cancels out the advantage described earlier. However, in the overall context of the various forces at play, it turned out to be advantageous to let the inner gates absorb at least part of the impact of the waves. Accordingly, the outer gates have been positioned only 3 metres above A.O.D., i.e. 2 metres lower than the inner gates,

which are 5 metres above A.O.D., so that in periods of very high water levels the outer and inner gates will take the force of the waves together. Part of the buffeting will be absorbed by the outer gate and part of each wave will spill over the outer gate and expend its remaining energy on the inner gate. This combination offers optimum resistance, both the outer gate and the Nabla beam will bear a lighter load than if the outer gate were to reach storm tide height and the inner gate were to serve merely as a standby for use in case the outer gate should get out of order or collapse under the wave attack.

Lastly, the inner gate had to be designed to withstand wave attack from the Haringvliet, i.e. from an easterly direction. This turned out to be the criterion for the design of the inner gates, for as they lean slightly towards the river, the lower waves from the Haringvliet impose greater stresses than the waves from the sea, even greater than the sea waves would impose on them if the outer gates were wide open.

Reference

1. *Model investigations on wave attack on structures.*
   M. A. Aartsen and W. A. Venis.
   Proceedings I. A. H. R. Congress 1959, Montreal.

2. *Wave impacts on the steel gates of a discharge sluice.*
   M. A. Aartsen, E. W. Bijker and W. C. Bischoff van Heemskerck.
   Proceedings I. A. H. R. Congress 1959, Montreal.

3. *Model investigations of wind wave forces.*
   J. E. Prins.
   Proceedings Coastal Engineering Congress, Scheveningen, 1960.

4. *Determination of the wave attack, anticipated upon a structure from laboratory and field observations.*
   W. A. Venis.
   Proceedings Coastal Engineering Congress, Scheveningen, 1960.

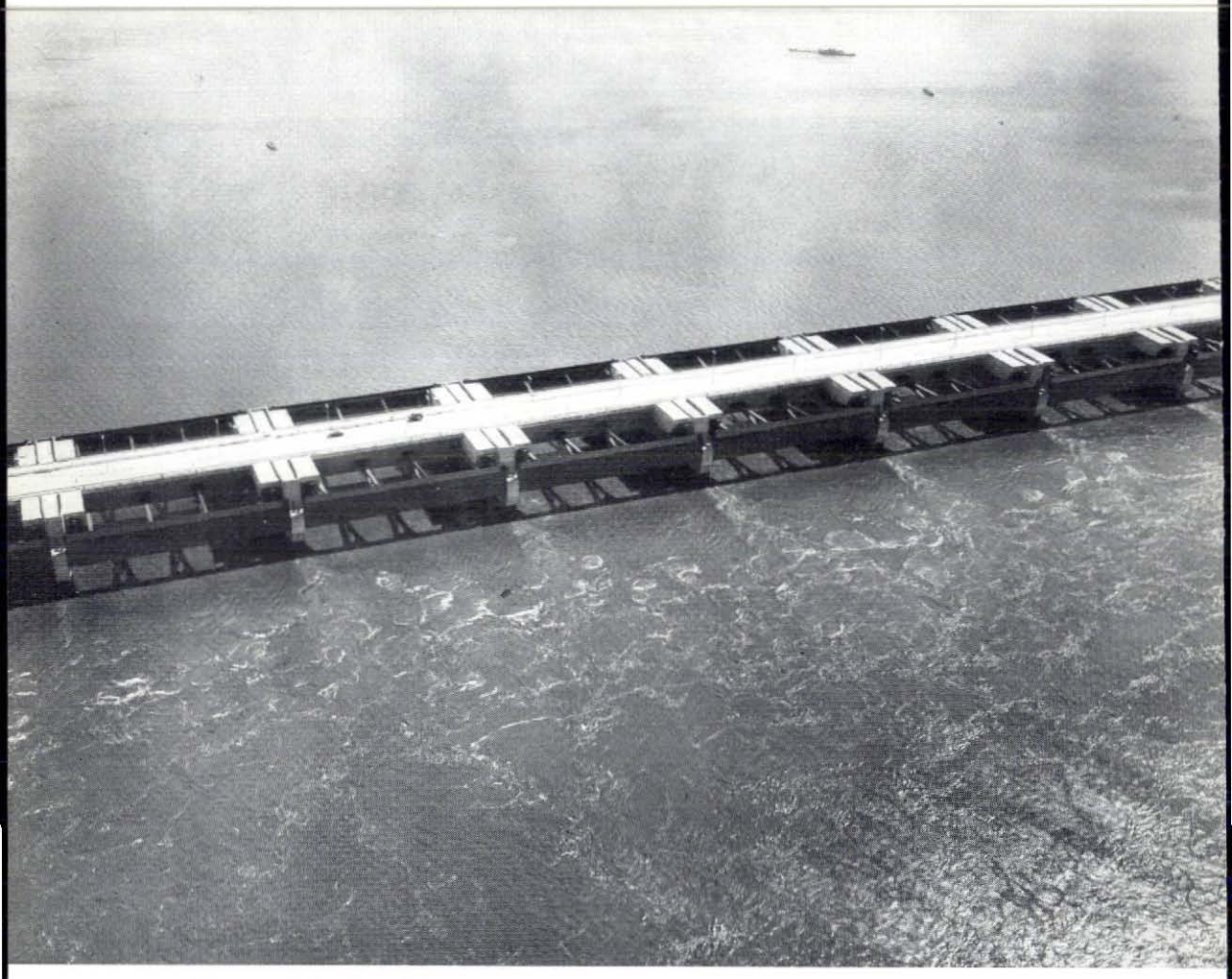

Photograph 2. Part of the sluice-gate complex with the seaward gates on the lower half of the picture (photo Bart Hofmeester)

II. The design of the sluice-gate complex

1. Introduction

As explained in section I, a big sluice complex had to be incorporated in the Haringvliet dam with a sill about 5.5. m below A.O.D.* and an overall width of over 1,000 m.

The sluice structure would have to carry a motor road and a road for small vehicular traffic. The openings between the piers had to be about sixty metres wide to allow ice to reach the sea in winter.

Alternative designs for the sluices are given in Figures 5, 6, 7 and 8. Lengthy study and research in the Hydraulics Laboratory and in the Laboratory for Technical and Physical Research (TNO) showed that the best and cheapest design was that given in Figure 6.

An artificial sunken island was made in the Haringvliet estuary with sand from the surrounding sea bottom (see Figure 9).

The dikes encircling the island were protected against wave attack.

The site was excavated for the foundations of the sluices and a temporary harbour was built on the leeward side of the island to accommodate the vessels bringing the materials to the site.

Figure 10 is a cross-section between piers. Figure 11 is a cross-section at the pier foundation.

The system has 17 openings; each opening is 56.5 m wide. Each of the sixteen piers is 5.5. m wide. The centre-to-centre distance is 62 m. The toes of the abutments for the dam proper, which will be built later, are 330 m apart.

The overall length of the system between the water sides of the abutments is 1,048.50 m.

The sill is 5.5 m below A.O.D. and on the river side it slopes 1 : 8 over a distance of 20 m.

On the seaward side there is a step 7 m deep to break the waves partially by causing them to strike a concrete wall, thus reducing the strain on the gates by about 50%.

As the subsoil consists of clay and soft sandy layers to depths ranging from 20 to 30 m below A.O.D. the sluice structure rests on 40 × 40 cm and 45 × 45 cm concrete piles. Sandy strata of adequate bearing capacity are found at greater depths.

Many of the piles are prestressed and some are reinforced.

The floor of the sluice both upstream and downstream is enclosed within coffer-

* Amsterdam Ordnance Datum (A.O.D.)

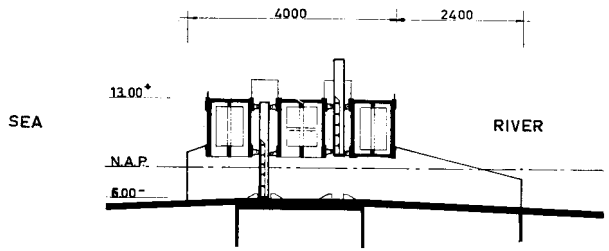

CROSS SECTION

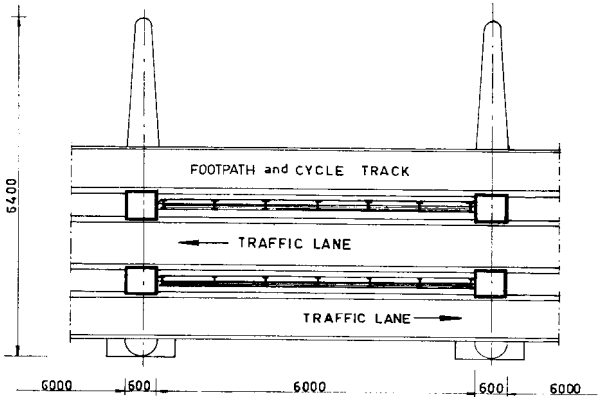

PLAN

Figure 5. Haringvliet sluice design 1

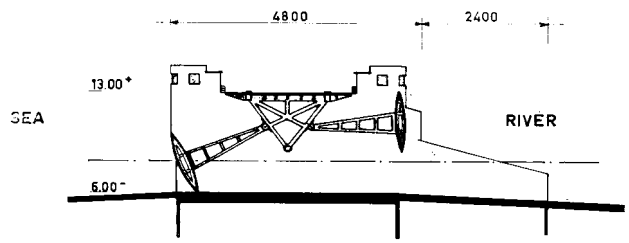

CROSS SECTION

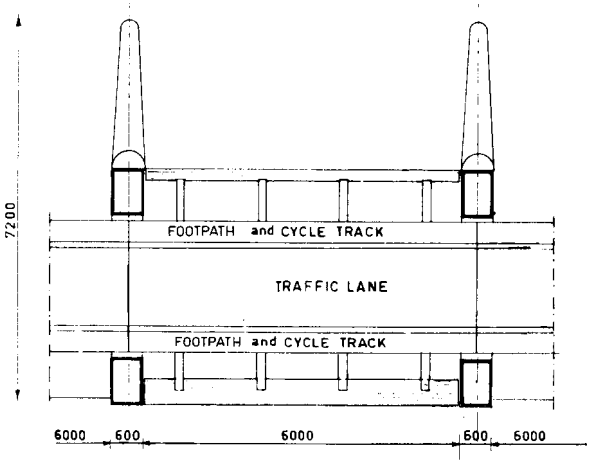

PLAN

Figure 6. Haringvliet sluice design 2

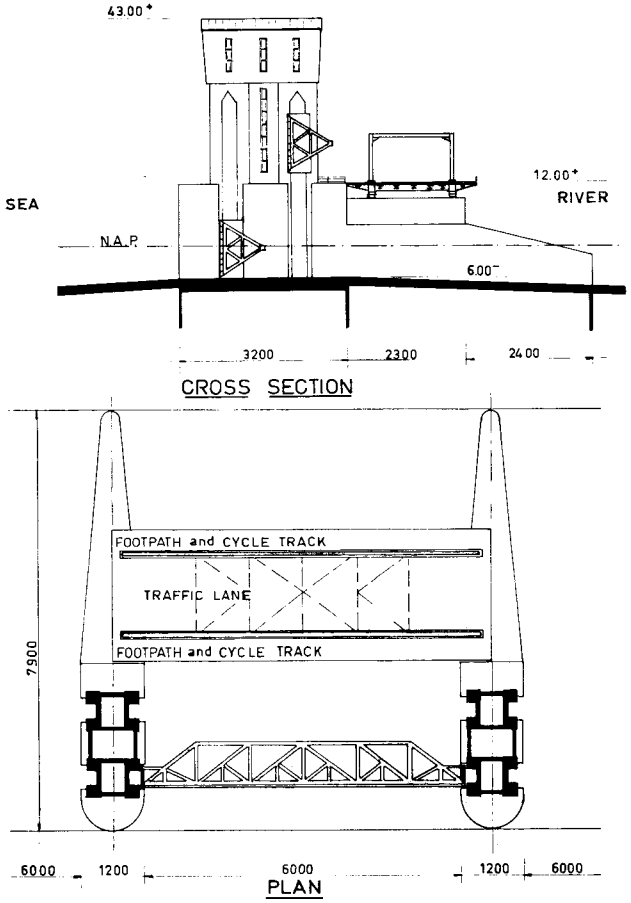

Figure 7. Haringvliet sluice design 3

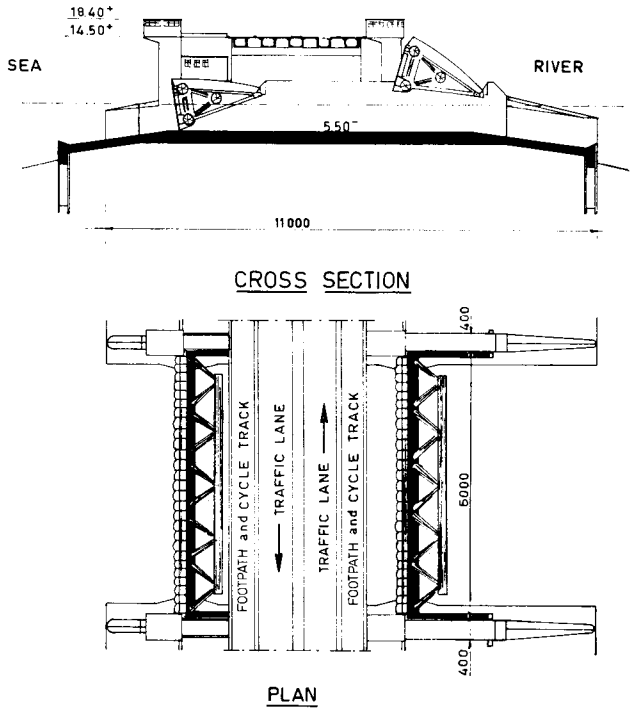

Figure 8. Haringvliet sluice design 4

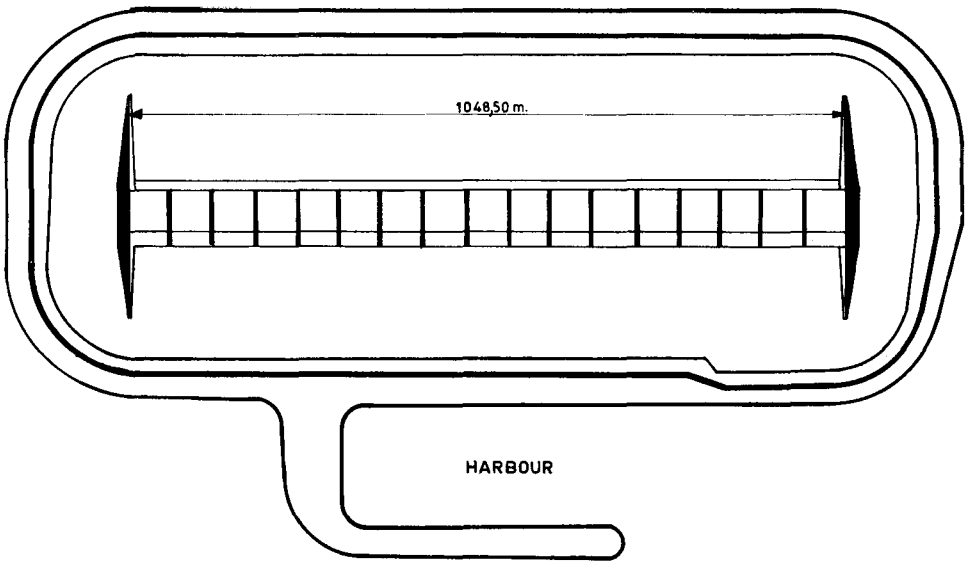

Figure 9. Excavations for the sluice foundations

dams made up of two walls of sheet-piling two metres apart with a filling of concrete between the walls.

The bottom on the seaward side of the sluice is protected with a concrete slab resting on piles and reaching 65 m seawards to a filter-bed, and on the river side with a thick concrete slab on a shallow foundation reaching 33 m upstream to another filter-bed.

The cofferdams are 92.52 m apart. Each opening between piers has two gates.

The outer gate can be looked upon as a breakwater and the inner gate as a second defence wall to take the excess volume during storm tides. To reduce the strain due to the waves, the outer gate has been made as low as the average summer water level would allow. The inner gate has been made high enough to take the excess volume during storm tides.

Provision is made for heating the walls of the piers next to the inner gates to enable the gates to be opened and closed when ice is coming down the rivers; the outer gate will then be open.

The gates are attached by means of arms to pivots fitted to a prestressed triangular hollow concrete beam. The arms are 15 metres apart. The top of the beam is covered with a concrete slab. The slab is insulated from the beam by a layer of asphalt to prevent the temperature of the beam from rising unduly when the sun shines.

The wings of the abutments rest on cofferdams, because a pile foundation, which would have been cheaper, was impossible to construct here in view of the great mass of the dike combined with the high horizontal stresses due to ground-water pressure.

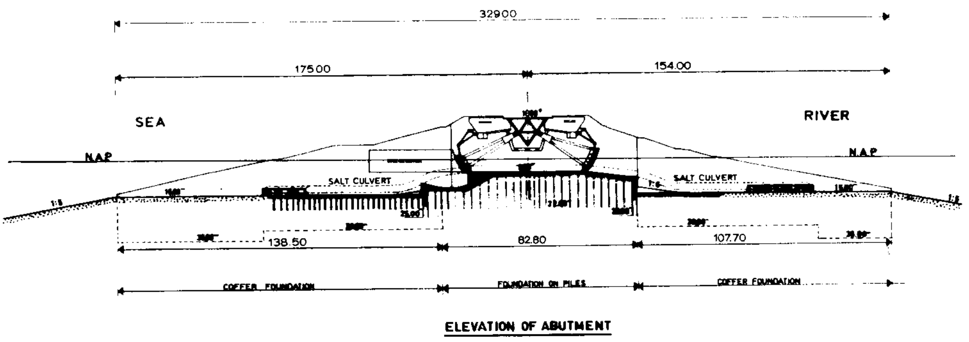

Figure 10. Abutment view of Haringvliet sluice

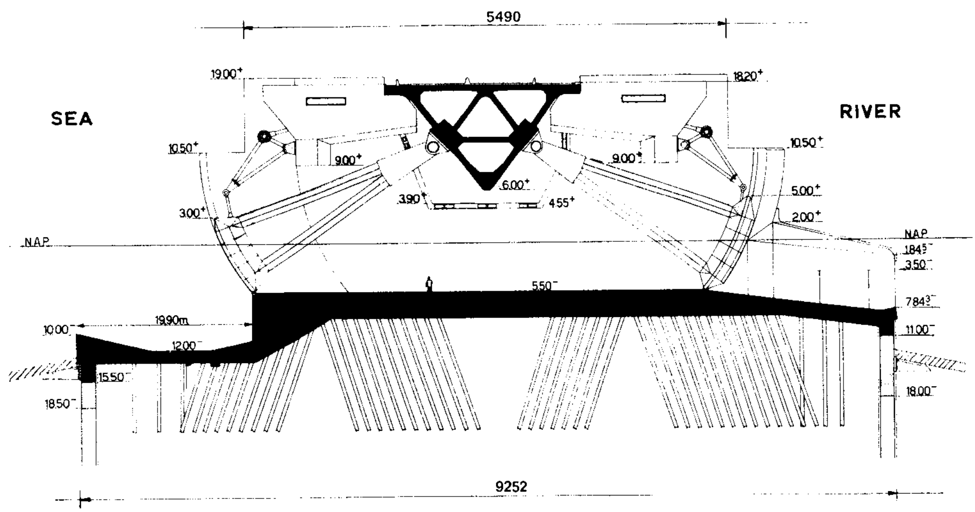

Figure 11. Cross-section of Haringvliet sluice at base of pier

The abutments are provided with toes, so that the resultant vector due to the maximum horizontal stress intersects the centreline of the foundation slab. This prevents the wall from being undermined by unequal soil pressure.

The abutments are provided with vents well below the surface of the water through which salt water may escape.

The intake velocity is controlled to prevent fresh water from being wasted.

There is a stilling box with columns on the seaward side of each abutment in which any waves that approach the structure obliquely can expend their energy.

There is a fishlock in every third pier to allow the fish that live in fresh water to come in from the sea.

Each pier has an ice saw on its upstream side; it consists of a steel blade fitted to the crest of a concrete buttress the top of which as a slope of 1 : 4.

The gates are lifted hydraulically.

Some of the problems that had to be solved when designing the sluice system are dealt with in this chapter. They pertained to:

the hydraulic and wave forces acting on the structure;
the foundations;
the design and construction of the hollow prestressed concrete beam;
research on concrete.

2. Forces acting on the structure

The stresses due to normal differences in water levels and due to vehicular traffic are very simple to find, but the stresses set up by wave attack gave rise to many design problems.

Since wave attack is a dynamic problem, we must take the total mass of the structure subject to attack and split up into a compound vibration system made up of the mass and elasticity of each gate, the mass and elasticity of the beam, the mass and elasticity of the piers and the elasticity of the foundation. (Figure 12.)

Experiments were conducted on a model in the Hydraulics Laboratory using wave trains in a variety of patterns impinging on the outer gates.

They showed that:

a. if the average water-level near the gate was less than two metres below the top of the gate, the impact of some of the waves might affect the structure;

b. if the average water-level near the gate was over two metres below the top of the gate, the impact of no wave would affect the structure;

c. the impact would be reduced by about 50% if there was a pocket in the bottom a short distance from the gates the depth of which was the same as that of the water immediately in front of the gates;

d. if the top of the outer gates, which at first was planned to be located at 5 m above average sea level, just like the inner gates, was brought down to 3 m above

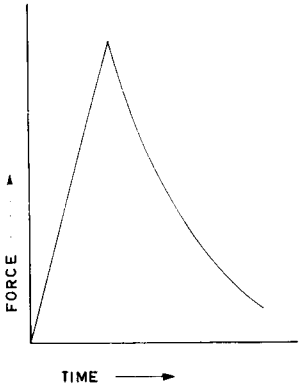

Figure 12. Example of wave impact shock-diagram.

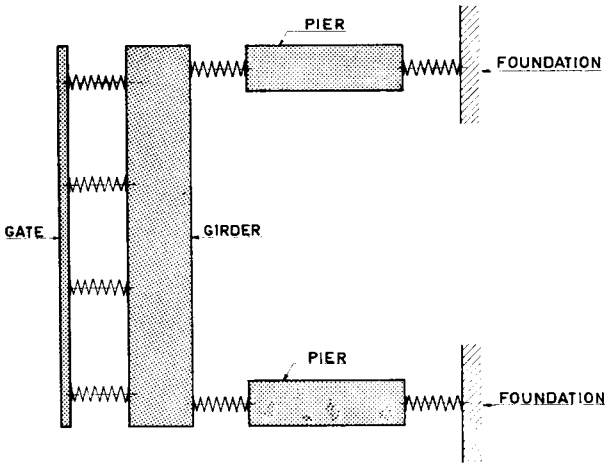

The compound vibration model of sluice

average sea level, the stresses would be reduced, and for three reasons;
the area attacked was smaller;
the waves in a body of water the level of which was 1 m above average sea level (i.e. the limit of impact) would be smaller than the waves in a body of water the level of which was 3 m above average sea level (i.e. storm tide level);
the percentage of shocks per wave was lower when the top of the gate was lower, consequently, that the frequency was smaller and that therefore the materials could be subjected to higher maximum stresses.

e. the tests for the shock diagrams were performed on a rigid wall; for a real impact it will make hardly any difference with an elastic construction, only the limit from the impacts is brought to a safer percentage;

f. the diagrams, that gave a shock impact were analized by the Fourier method and brought on the construction. The calculation was made by a computer and controlled by an electric analogan;

g. the vibration periodicity of the foundation was so short, that the most violent wave attack produced no dynamic effects, so the system was a compound vibration of the gate mass-elasticity and the beam mass-elasticity.

The experiments conducted in the Hydraulics Laboratory to determine the optimum design of the inner gates when the outer gates are open during storm tides showed that the waves would break on and overtop the long bottom slab before they reached the gates themselves.

So the forces acting on these gates would be much lower than those acting on the outer gates.

The waves acting on the river side gates are small and the stresses they set up are slight.

3. The foundations

The pile foundations fall broadly into two groups;
the piles under the bottom slabs. As a rule, they are subjected to compression but under certain circumstances they are under tension;
the piles under the central abutment sections and under the piers. They are constantly subjected to compression ranging from zero to a certain maximum, though for about 95% of the time they have to withstand about 2/3 of the maximum pressure.

To find the maximum bearing capacity it was necessary to draw up a comprehensive research programme for the 30,000 piles to be carried out by the Soil Mechanics Laboratory and the Technical Research Institute.

3.1. Piles subject to tension

A model was made in which to test shear distribution around a pile subject to tension driven into fine-grained soil (see Figure 13).

An unstressed steel strip was embedded in a plexi-glass plate. The plate itself was then cemented to a very stiff lower girder.

The maximum force used in the model was about 100 kg. The isochromes and isoclines were recorded while the stress was being applied. Then, from the formula

$$\tau = \frac{\rho_1 - \rho_2}{2} \sin 2\varphi$$

in which

τ = shear stress

$\rho_1 - \rho_2$ = difference between the main stresses found on the isochrome recording, τ can be found by the shear-difference method. For a plain stress distribution

$$\frac{\delta\sigma_x}{\delta x} + \frac{\delta\tau}{\delta y} + x = 0 \qquad \frac{\delta\sigma_y}{\delta y} + \frac{\delta\tau}{\delta x} + y = 0$$

If X and Y as mass forces are disregarded, we get

$$\sigma_x = (\sigma_x)_0 - \int \frac{\delta\tau}{\delta y}\, dy \qquad \text{and} \qquad \sigma_y = (\sigma_y)_0 - \int \frac{\delta\tau}{\delta x}\, dy$$

or

$$\sigma_x = (\sigma_x)_0 - \sum \frac{\Delta\tau}{\Delta y} \Delta x \qquad \text{and} \qquad \sigma_y = (\sigma_y)_0 - \sum \frac{\Delta\tau}{\Delta x} \Delta y$$

for the free edge; $(\sigma_x)_0$ and $(\sigma_y)_0$ are known and the stresses σ_x and σ_y at every point can then be calculated.

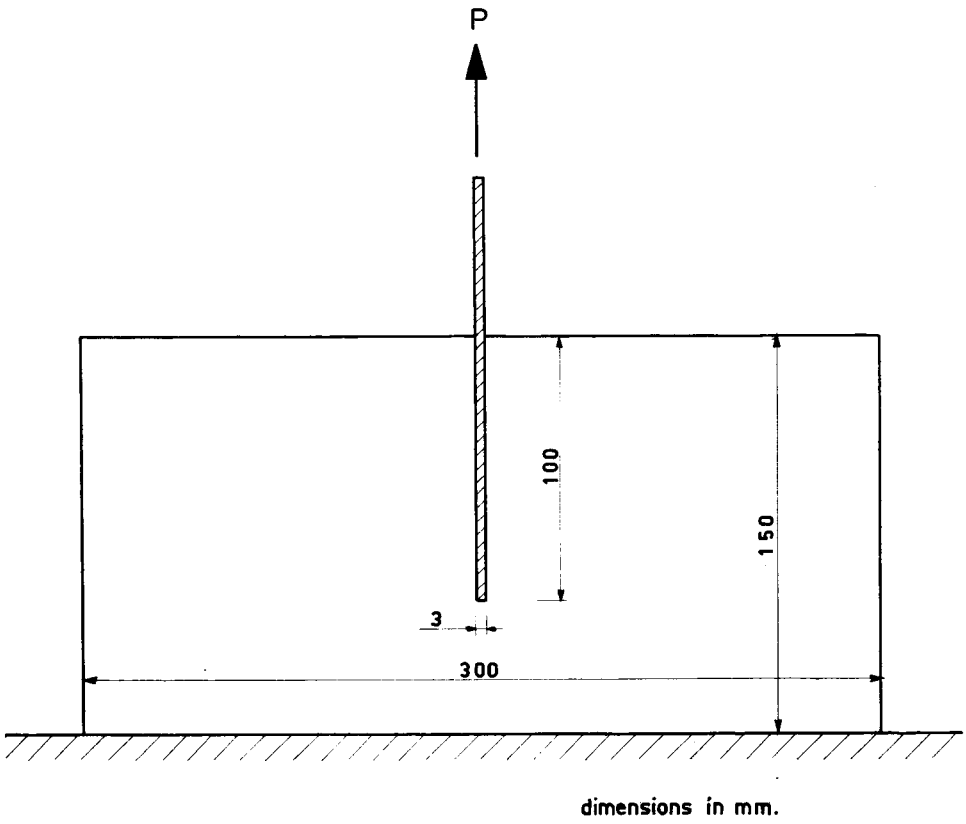

Figure 13. Model of tension pile embedded in an elastic medium

The shear stress was seen to be very high near the foot of the pile as force P increased.

After this experiment, a standard reinforced pile, a steel pile and a prestressed concrete pile were driven into the soil near the site of the sluice-gates. Another reinforced concrete pile was driven into the soil, water jets being used to loosen the soil and annihilate surface friction down to about 1 m from the foot.

The piles were of the same lengths and in the same layers as shown in the drawings.

The piles were fitted with electrical instruments for measuring elongations.

The piles were subjected to stresses of various kinds, viz. rapidly alternating compression and tension, protracted tension, tension at varying intervals, and so on.

Shear stress was found to be concentrated near the foot of the pile, as it was in the test model, and by and large two thirds of the tensile strain can be said to be taken by the foot of the pile.

The shear distribution is shown in Figure 14.

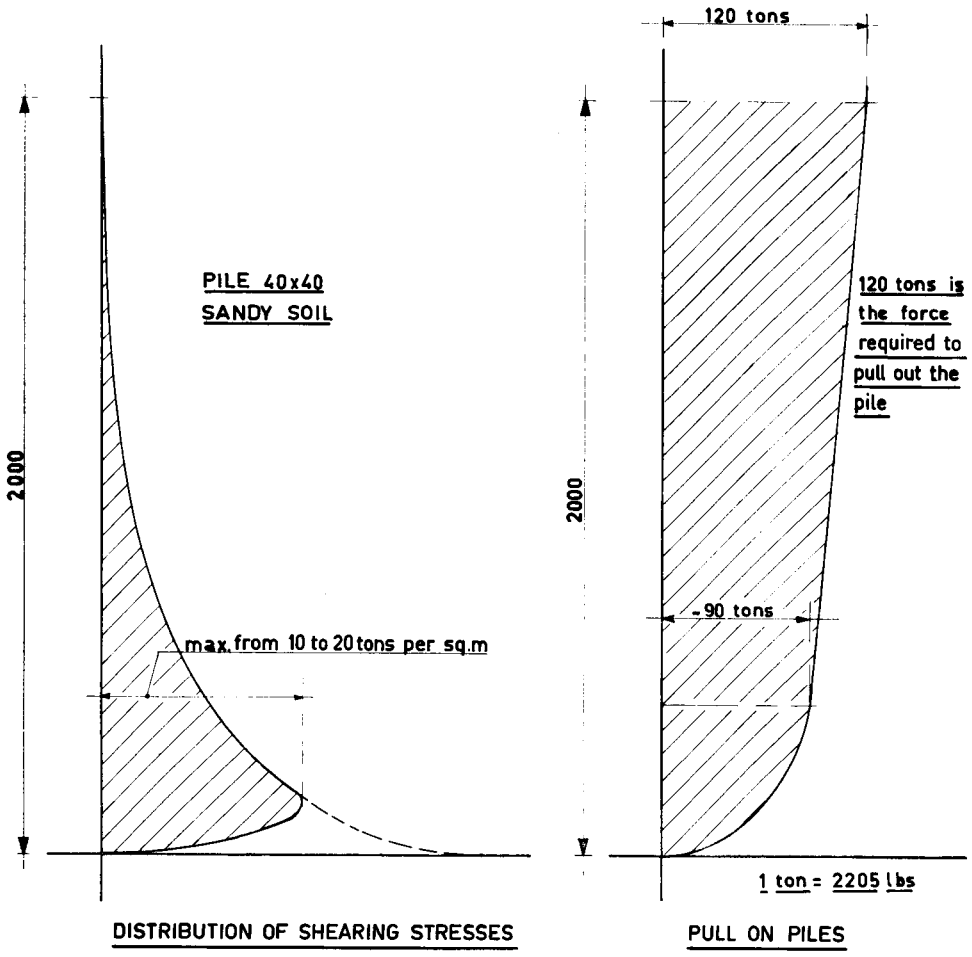

Figure 14. Diagram of shear distribution resulting from the model shown in Figure 13

In spite of the fact that the results of the experiments afforded an insight into the behaviour of tension piles, exact calculation of the distribution of forces along the pile is not yet possible, while the differences between the elongation of the pile and the displacement of the surrounding soil are unknown. The experiments showed that there is a certain amount of slip between the soil and the surface of the pile. The other boundary conditions are known.

As the second allowable limit of tension is marked by the rising of the foot of the pile and the effect of the rise under changing loading conditions, this had also to be studied with the aid of the experimental piles.

Also it was necessary to test the rise of a group of piles and compare it with that of a single pile.

When a group of piles is extracted, there must obviously be a line in the soil between the piles along which the shear stresses are zero. The line will be an axis of symmetry. The shear stresses around a single pile are more widely distributed than those around a close-set group of piles and it is clear that the bearing capacity of a single pile can be greater than that of a single pile belonging to a group.

The maximum bearing capacity of a pile belonging to a group is limited by the weight of the soil column belonging to that pile.

A tension of 35 tons per pile was regarded as reasonable in the light of these considerations.

3.2 Piles subject to compression

Stresses will be applied to and removed from the piles on which the piers rest relatively quickly when waves pound the gates but there will be hardly any variation in pile stresses under normal circumstances.

To determine the effect of variations in stress on bearing capacity, some piles were driven in the same spot as the experimental tension piles and stresses were applied to and removed from them in rapid succession. The displacement of the heads of the feet of the piles were recorded to find the deformation bearing capacity.

To find the maximum bearing capacity the stress applied was increased until there was major displacement of the pile.

The terminal deformation bearing capacity was 135 tons.

The admissible maximum bearing capacity was 75 tons. This figure can be split up into two parts, about 25% is borne by the foot of the pile and 75% is borne by friction.

As the stress increases, the percentage borne by the foot of the pile rises to about 60% and that borne by friction drops to 40% until the maximum of 135 tons is reached.

Friction reaches a maximum value of 0.4×135 tons $= 54$ tons for a pile 13 m long and a surface area of $13 \times 1.6 = 20$ sq.m. The average friction limit is about 2.7 tons per sq.m.

When the experiments had been completed, the pile foundation for the piers was designed and a group of about 50 piles was driven as quickly as possible. One pile in the middle of the group was loaded to test the effect of compression.

The pile was subjected to a stress of 200 tons, dependent on the installation and there was hardly any deformation.

The displacement of the foot of the pile was found to be 0.2 mm after the stress had been changed from 45 to 97 tons and back again very rapidly about 200 times.

It became clear that a group of piles behaves as if it were a single big pile and that the calculated admissible bearing capacity of the group of n piles could be set at $n \times 90$ tons. This explains the special arrangement of the groups of piles supporting the piers.

The elasticity of a single pile including the subsoil had to be determined to find the elasticity of the entire pile foundation in the light of the conclusions in paragraph 2.g regarding the calculations for the whole structure when subject to wave action.

It was about 200 tons per cm for stresses ranging from 40 to 60 tons.

For the pile in the group this was about 700 tons per cm for loads varying from 45 to 90 tons.

It is impossible to give an exact figure for the arrangement finally decided upon because it was impossible to test the whole group of piles. Nevertheless, the elastic limit of each group of piles had to be ascertained before their periodicity could be calculated. Not less than 200 tons per cm was taken as the lower limit because the effects of the foot pressure of a group of piles extend much deeper than those of the foot pressure of a single pile but the friction between a single pile in a group and the surrounding soil will be lower than that of a single pile.

A stress of 200 n tons per cm was taken for n piles.

4. The construction of the hollow triangular prestressed concrete beam

At intervals of approximately 15 m the arms of the segmental sluice gates are hinged to prestressed concrete girders of hollow triangular section called Nabla girders (Figure 15).

Each of these girders is 60 m long, 22.4 m wide and 12 m deep; the outside triangular part has a wall thickness of 60 cm and the inside triangular part is 50 cm thick.

The top serves as a bridge deck for vehicular traffic.

Some of the principal static stresses equivalent to the dynamic wave stress combinations to which these girders may be subjected are shown in Figure 16.

In view of the great importance of the structure concerned and in order to minimize the risk of the reinforcing steel corroding, it was laid down that no principal tensile stresses should occur when these loads were acting on the structure.

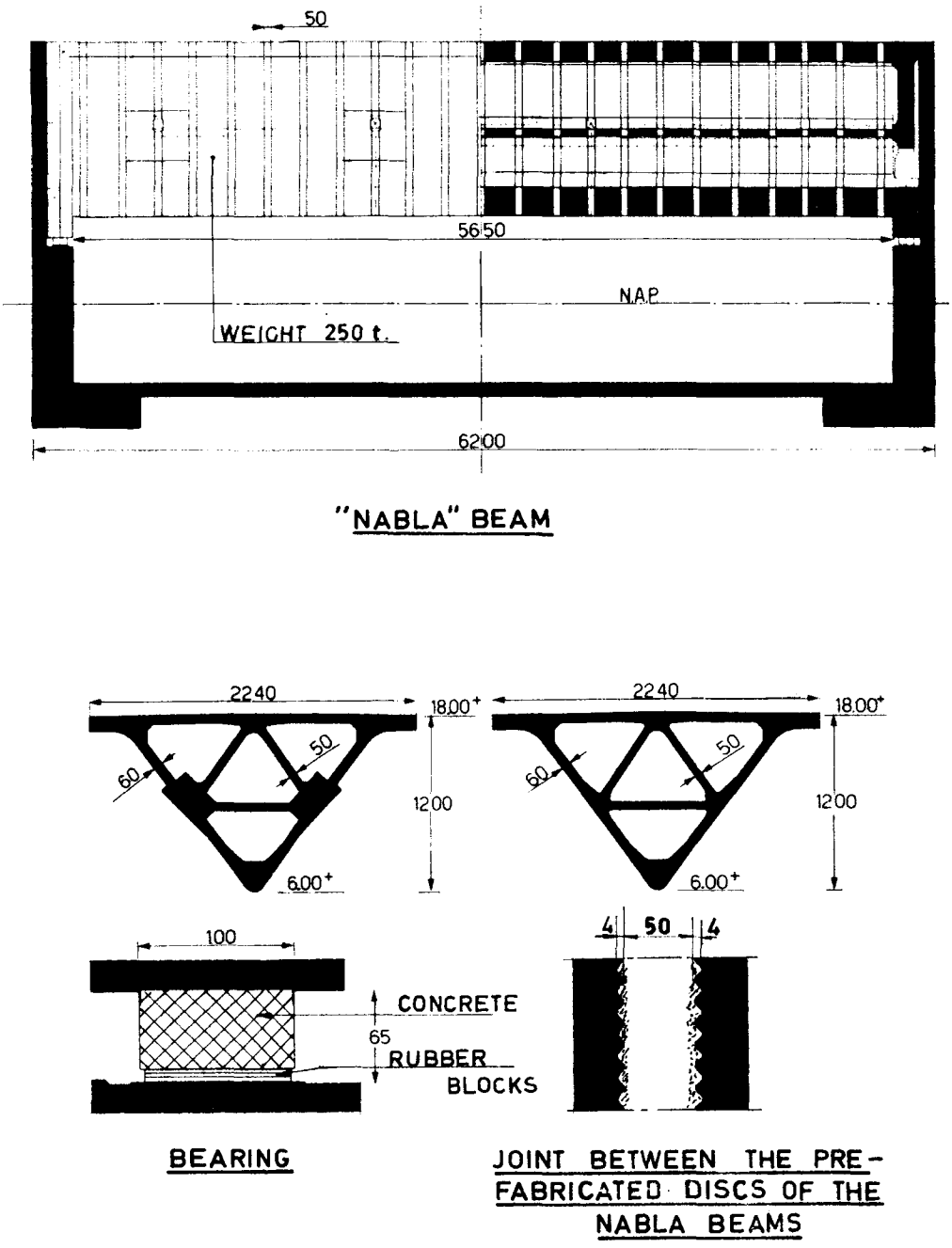

Figure 15. Joint between two prefabricated Nabla beam sections

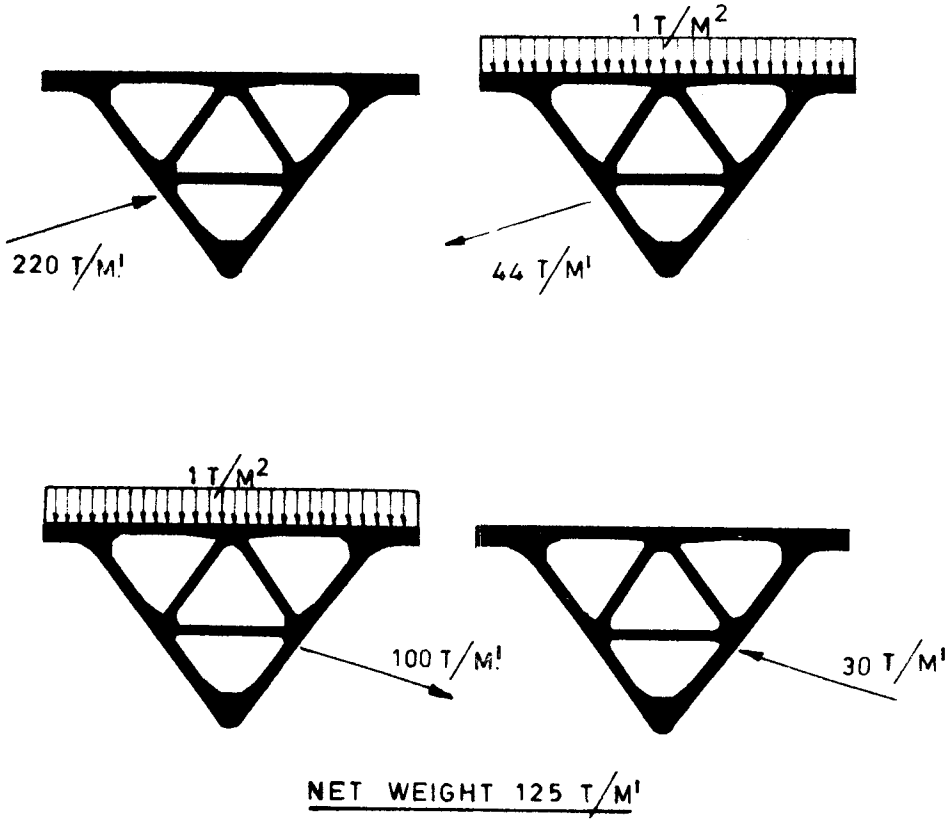

Figure 16. Loads on the Nabla beam transformed from the dynamic impact

It was also postulated that at 1.3 times the basic stress the principal tensile stresses should not exceed 10 kg per sq.cm. (so as to preclude cracking in the joints) and that the factor of safety should be not less than 2.2.

The ends of the girders rest on the piers, sheet rubber cushions distributing the weight.

As it would have been very difficult indeed to construct and position such huge prestressed concrete beams in one piece, it was decided to build them up from precast units weighing 250 metric tons each, 22 units forming one girder. They were positioned on temporary supports by a crane specially built for the job.

The longitudinal prestressing cables were then threaded through the 22 units and the joints between the units (50 cm wide) concreted.

The longitudinal and transverse prestress was applied when the concrete in the joints had hardened and the temporary support was then removed.

Each girder contains 3,500 cub.m. concrete, 240 tons prestressing steel and 200 tons of "highbond" steel.

The size and the method of constructing these beams and the stresses to which they were to be subjected gave rise to a number of special problems, some of which were solved by experimental means. On completing the plans, it was considered necessary to verify the accuracy of the results of experiments and test the theories underlying the design. Accordingly, tests were carried out on a 1 : 15 scale model incorporating every detail that might affect the process of construction contemplated.

4.1 Structural calculations and prestressing

Broadly, the stresses due to water pressure are distributed throughout the girder in the following manner:

The concentrated stresses at the pivots of the gates (up to 3,300 tons per pivot) are transmitted to the internal triangle through the locally enlarged concrete section behind the pivots.

The load, which takes the form of shear stresses, is distributed throughout the internal triangle which then passes them on to the external triangle.

The external and internal triangles, acting together as a girder, transmit the forces to the end diaphragms.

These are the principal stresses but the cross-section is also subjected to bending moments due to the structure's own weight, the live load and eccentric angular forces. Allowance had also to be made for changes in temperature, wind stresses and any differences in the settlement of the piers.

Two of the questions that had to be answered when preparing the structural calculations were:

Do the characteristics of this type of girder accord with the conventional beam theory in the matter of its proportions and the stiffness of the end cross-section?
How are the shear stresses around the pivots distributed?

Stress readings were taken on a steel 1 : 100 scale model fitted with transverse strengtheners at the pivots instead of the internal triangle. The stresses were found to differ from those calculated in accordance with the beam theory by about 10%. A calculation based on the plate theory exhibited similar differences.

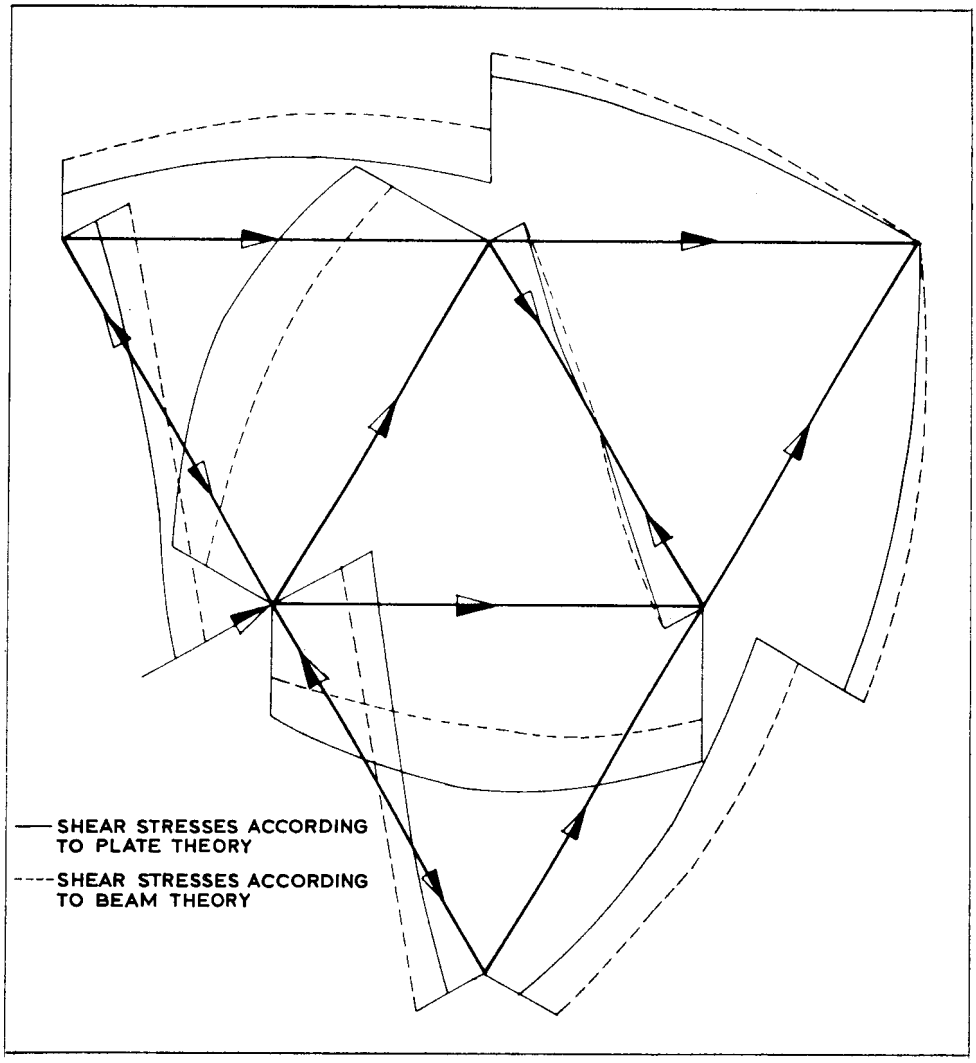

Figure 17. Comparison of shear-stresses obtained from the two alternative theories

Accordingly, the structural calculations were prepared in accordance with the conventional beam theory, the values of the section moduli being appropriately corrected on the basis of the tests and calculations described above. Not until much later was it decided to incorporate the triangular internal stiffener throughout the length of the girder. As the 1 : 15 scale verification test described later shows, the beam theory is still applicable almost in its entirety to the modified design.

When analysed according to the plate theory, the distribution of shear stresses around the end diaphragm was found to differ considerably from the values determined on the basis of the beam theory (see Figure 17).

Heavy shear stresses occur in the deep, thin walls of the Nabla girder. The maximum shear stresses under working load are 35 kg per sq.cm. for an average normal stress of 55 kg per sq.cm. set up by the longitudinal prestressing.

The principal tensile stresses are completely cancelled out by the longitudinal and transverse prestressing.

It was feared that, because of the relatively small area of the compression zone in the concrete at the failure stage (see Figure 18), the ultimate strength would be determined by the shearing of the concrete along the faces between the precast units and the concrete in the joints. The shear strength depends very largely on the profile of the joint and for this reason a series of shearing tests were carried out; they are described in this chapter.

As regards temperature, the following points should be noted:

There is almost constant difference in temperature between the internal and external faces of the walls due to temperature variations occurring with a frequency of several weeks.

Similar variations, but with a frequency of one day.

Similar variations, but with a frequency of only one hour or a few hours. The variations have the most marked effect, tests having shown that an abrupt difference in temperature of as much as 25 °C. may occur in concrete exposed to direct sunshine.

As the sluice structure runs in a north-south direction, the sides of the girder will be in the shade nearly all the time. The top surface of the girder is exposed to direct sunshine, however, and to shade the actual structure from the heat of the sun, an independent concrete deck, 18 cm thick, serving at the same time as the road surface, was placed on top of the girder. This will reduce the stress set up in the top slab by sudden temperature variations to 15 kg per sq.cm.

The longitudinal prestressing is produced by 193 cables, each composed of fifty-four 6 mm diameter rods exerting a permanent prestressing tension of 136.8 tons per cable. The B.B.R.V. prestressing system was adopted for these cables. The cable ducts in the individual precast units are straight, the curvature of the cables as a whole being obtained by slight changes in direction at the joints.

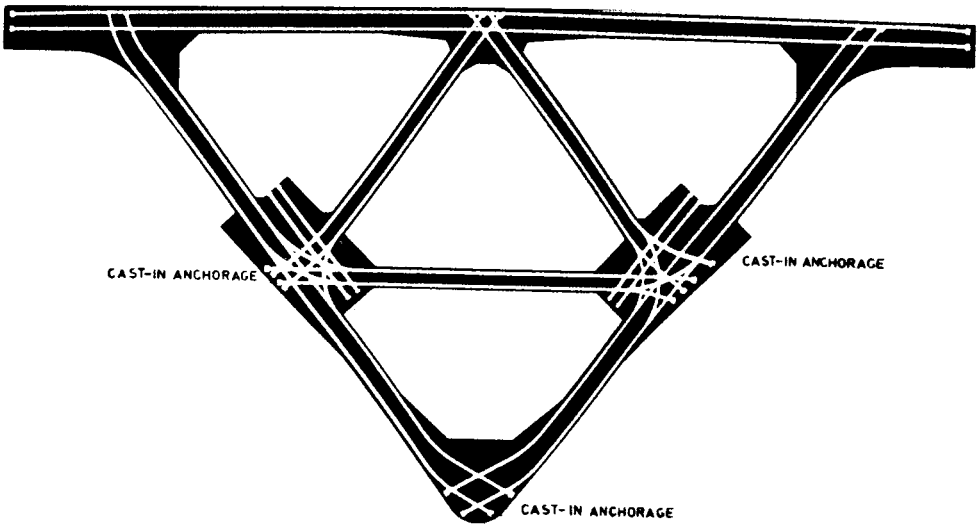

Figure 18. Transverse lay-out of steel cable

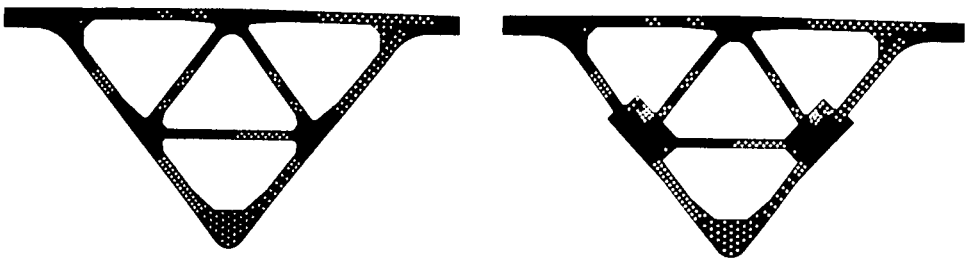

Figures 19 and 20. Longtitudinal lay-out of steel cable in the centre section of the beam

In order to determine the frictional losses due to the change of direction and due to possible dimensional inaccuracies, a full-scale test was carried out, which showed that $\mu = 0.32$ if an additional angular change of $K = 0.006$ rad per m was assumed to occur.

Transverse prestressing is produced by Freyssinet cables, each composed of twelve 7 mm diameter rods, exerting a permanent prestressing tension of 43.2 tons per cable. There are about 1,100 transverse cables per girder.

The transverse prestressing has three functions:

- to prevent the occurrence of tensile stresses due to shear stress;
- to resist tensile forces in the transverse direction especially in the vicinity of the pivots;
- to resist the secondary bending moments in the side walls and top slab.

It was impossible to reduce the prestressing by adapting the cable profiles to the bending moment distribution, because the central part of the top slab and sides had to be kept free of obstructions to allow the longitudinal prestressing cables to be fitted.

The requirement that all the cable anchorages in the external walls except those located behind the pivots and in the top slab must be cast in "dead-end" anchorages very largely conditioned the arrangement of the transverse prestressing cables.

To obtain the correct transverse prestressing in all parts of the walls of the internal and external triangles, the cable arrangement shown diagrammatically in Figure 18 had to be adopted.

The ducts for the longitudinal cables (the overall profiles of which are as nearly as possible parabolic) are shown in Figures 19 and 20.

Figure 19 shows a typical cross-section in the centre of the girder, where most of the cable concentration is found on the river side. Figure 20 is a cross-section at the pivots showing the local stiffening of the section which serves as the anchor block for these pivots and corrects the eccentricity of the support-arms as much as possible.

The transverse prestressing cables decribe an angle of 72°30′ or 53° at the junctions between the component slabs of the girder. Because of the restricted space, it was not possible to exceed a radius of curvature of about 1.75 m.

This gave rise to the question whether this radius was not too small.

Tests showed that this small radius did not cause any greater frictional losses than a normal radius would have done. Only the angle affects the friction. The radius sets up additional bending stresses in the strands.

4.2 Transmission of shear at joints

There is not much literature on the subject of the transmission of large shear forces by joints. The literature there is relates mainly to joints in which the ratio of shear force to direct force is below 0.7, or to joints that only transmit a small shear stress.

In the present case, however, there is a direct force of considerable magnitude and a relatively large shear stress.

Tests had to be carried out to discover whether the direct forces and the shear force acting there could be transmitted by suitably profiling the faces of the joint.

First a series of tests was conducted with a view to determining the optimum profile.

In addition, a test was conducted on a mock-up of the joint surface of a Nabla girder, duly provided with joints. The test was carried out for the stress-combinations that would occur in actual practice (i.e. prestress in two directions, bending moments and shear).

4.2.1. Profile of joint surface

The effect of stresses acting on the profile of the joint surface was investigated by carrying out tests on specimens considerably scaled down.

Concrete was placed between two precast, steam-cured concrete blocks (see Figure 21), the joint faces of which had been shaped to a certain profile. When the concrete in the joint had hardened, a stress corresponding to 7.5 kg per sq.cm. within the joint was applied by means of a spring.

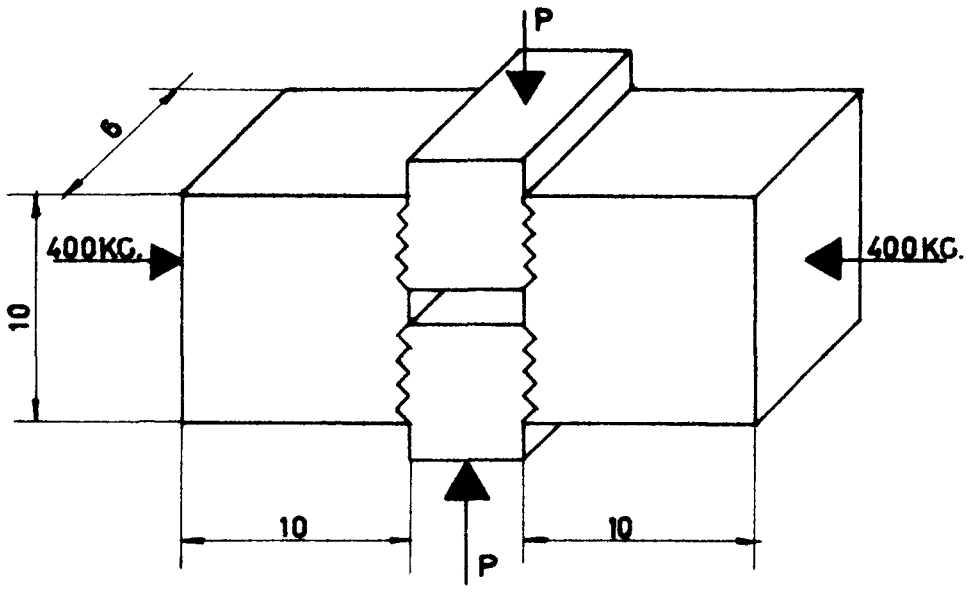

Figure 21. Profile-test of the joint

The cube strength of the precast concrete and the joint concrete was 400 kg per sq.cm.; the maximum particle size of the aggregate was 10 mm.

The tests yielded the following results:

Profile of joint face	Force P (kg) producing failure
Pyramidal configuration 1 × 1 cm 1.5 mm high	1,403 kg
Pyramidal configuration 0.6 × 0.6 cm 1.0 mm high	1,470 kg
Of 3 mm Sinusoidal corrugations at right angles to direction of shear	1,080 kg
Cast against diamond chequer plate	810 kg
Smooth	670 kg

In none of these tests was failure preceded by crushing of the precast concrete or the concrete in the joint; in all cases the latter concrete had merely become disengaged from the profile. It seemed that a more deeply indented profile would give better results and for this reason a second series of tests on larger specimens was carried out. The test set-up was broadly similar to that adopted for the first series but this time the precast concrete blocks were 60 × 60 × 25 cm, while the transverse stress was produced by means of a 26 mm diameter Dywidag prestressing bar.

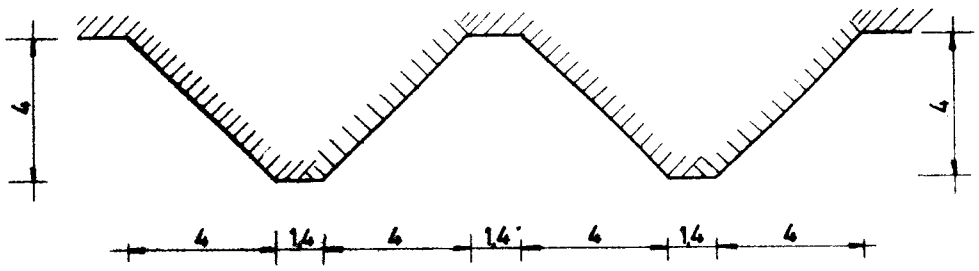

Figure 22. Joint design

The stress was maintained throughout the test at a constant value of 31.25 tons with a jack and a load cell, thus prestressing the test joint to 25 kg per sq.cm. The maximum particle size of the aggregate was again 10 mm; the cube strength of the precast blocks was approximately 525 kg per sq.cm. and that of the joint concrete was approximately 500 kg per sq.cm. The following results were obtained:

Profile of joint face	Force P (tons) producing failure	Average shear force or direct force
a. Cast against rubber mat with pyramidal features 1 × 1 cm, 1.5 mm high	55 45 64	1.75
b. Cast against steel sheet with 4 cm teeth at right angles to direction of shear	94 91 94	3.00
c. Same as b, but pressed into top layer after concrete had been cast	91 100 91.5	2.92
d. Cast against steel sheet with pyramidal features 2.7 × 2.7 cm, 3-4 mm high	47.5 65 63	1.87
e. Cast against Métal Deployé No. 82 (expanded metal) with a 1.5 × 2.5 cm mesh	92.5 90 91.1	2.92

The results obtained with profiles a and d differed considerably from those obtained with the others.

Profiles a and d were shallow in relation to their base dimensions and had "flat" slopes; the failure pattern was similar to that in the first series of tests and there was no crushing of the concrete.

On the other hand, the other types of profile were more deeply indented and had steeper slopes: entire particles of gravel penetrated between the features of the profile and failure occurred because the concrete was crushed in a plane which did not quite coincide with the plane of the joint. The failure load was, therefore, a good deal higher than it was for the "shallow" profiles.

In view of the above results, and having regard to the maximum particle size of the aggregate to be used in the concrete for the actual structure, the shape shown in Figure 22 was adopted for the joint profile.

4.2.2. Shear test on joint surface of Nabla girder

When the most favourable profile had been determined by means of the tests described above, the next step was to find out whether the walls of the girder with its joints could indeed transmit the combinations of bending moments and shear forces that were likely to occur in reality.

Under normal conditions the stress distribution in the joint at the central pivots is as follows:

direct stress at bottom	5 kg per sq. cm.;
direct stress at top	107 kg per sq. cm.;
maximum shear stress	37 kg per sq. cm.

A simplified mock-up of a wall of the Nabla girder was constructed as shown in Figure 23.

The top and bottom flanges represented the local stiffening of the section at the junctions of the walls of the actual girder. As in the structure itself, the wall was assembled from individual units precast in steel moulds and steam cured. The joints between the units were then concreted and vertical and horizontal prestressing applied.

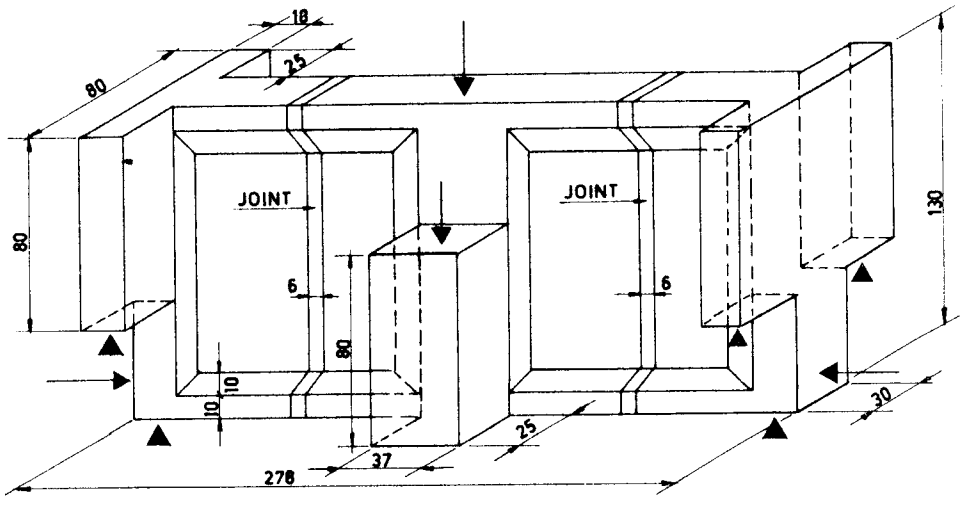

Figure 23. Model for testing joints

When testing these specimens efforts were made to gain some information as to how the following factors affected the ultimate strength:

- the quality of the work;
- whether or not the mild-steel reinforcement was made continuous across the joints;
- tensile shrinkage stresses in the joints.

Some of the experimental arrangements adopted for testing the seven specimens were: an ideal joint (conceived as a dummy joint) and a very poor joint (filled with low-strength concrete); the mild steel was extended across certain joints and omitted in others and in some of the joints tensile stresses due to shrinkage were simulated by vertically prestressing the precast units first and then concreting the joints.

The vertical prestressing was protected by means of 7 mm diameter wires and amounted to 26 kg per sq. cm., just as in the walls of the actual Nabla girder.

The longitudinal prestressing was applied by means of four Dywidag bars and was 110 tons at failure, corresponding to the average compressive stress of 58 kg per sq. cm.

Specimen	Dummy joint	Quality of joint	Mild steel reinforcement continuous in joints	Joint without prestress	*Cube strength* kg per sq. cm.		P ultimate in tons	*Maximum shear stress* Average stress referred to the uncracked section
					pre-cast unit	joint		
I	x				440	440	200	1.94
II	x		x		570	570	270	2.38
III		good			516	544	247	2.19
IV		moderate		x	462	268	188	1.70
V		good	x		445	492	209	1.85
VI		good		x	454	522	239	2.11
VII	x				400	400	265	2.01

Specimen I is not comparable with the others. The beam failed in the bending test because the prestressing cables had been placed too high.

The first shear cracks appeared in all the beams when the load was between 90 and 100 tons, irrespective of the type of joint. The cracks appeared near the joint in the centre of the beam and were at 40° to the horizontal.

The principal tensile stress at cracking point was approximately 12 kg per sq. cm. but the tensile strength of the concrete as determined by means of the indirect test was 29-39 kg per sq. cm., depending on the quality of the concrete used.

The discrepancy was explained by the occurrence of high shrinkage stresses, which were partly due to the presence of the particularly heavy reinforcement (400 kg steel per cubic metre of concrete).

Vertical (flexural) cracks appeared on the lower edge of the specimens at loads between 150 and 200 tons (specimens I and II), at between 75 and 107 tons (specimens III and IV).

This shows clearly that this type of cracking is very largely due to the presence of a joint. The difference is probably attributable to the low bond strength between the concrete in the joint and the precast concrete.

The test did not show that the continuity of the mild-steel reinforcement across the joint had any effect on the ultimate strength but the safety factor of the Nabla girder is much higher when the mildsteel reinforcement is continuous and constitutes a more or less unbroken frame.

When the load was increased, the cracks at 40° became wider and more numerous. Failure was attended by the extrusion of a wedge from the compression zone and shearing at or near the joint; indeed, shearing had to occur because there were many buckled reinforcing bars in the concrete on either side of the joint.

4.2.3. Verifying the design with a model test

The complexity of the structure made it necessary to investigate its behaviour with a model to verify the boundary conditions established by means of the subsidiary tests.

As the investigations were to cover not only the elasticity but also the cracking and failure points, the model had to be as realistic as possible, i.e. not only the dimensions but also the properties of the concrete and steel had to correspond to those of the actual structure. The model had to be of a reasonable size so that it could be made to include adequate detail; too large a model on the other hand would have made it impossible to keep the forces that had to be applied within reasonable limits (totalling roughly 200 tons at failure). It was decided to set the scale factor n at 15.

The phenomena that occur in the actual structure can be reproduced in the model by dividing the forces acting upon the prototype by n^2. The stresses due to the weight of the model itself, however, decrease in proportion to n^3 (i.e. in proportion to the volume).

To obtain the correct stresses due to the weight of the structure, it is therefore necessary to apply an additional load equal to (n-1) times that of the model. For the top slab of the girder this compensating load was applied by means of a system of levers; for the rest of the girder it was applied by an arrangement of tension springs.

Forces corresponding to the compressive and tensile forces acting upon the pivots on the two sides of the structure (i.e. the side facing the sea and the side facing inland) were applied by means of hydraulic jacks. The magnitude of these forces was measured with the aid of dynamometers. The live load on the top slab was also applied by the system of levers. Furthermore, such rotation of the piers as might occur in consequence of the settlement of the structure was reproducible in the model.

The loading diagram is shown in Figure 24.

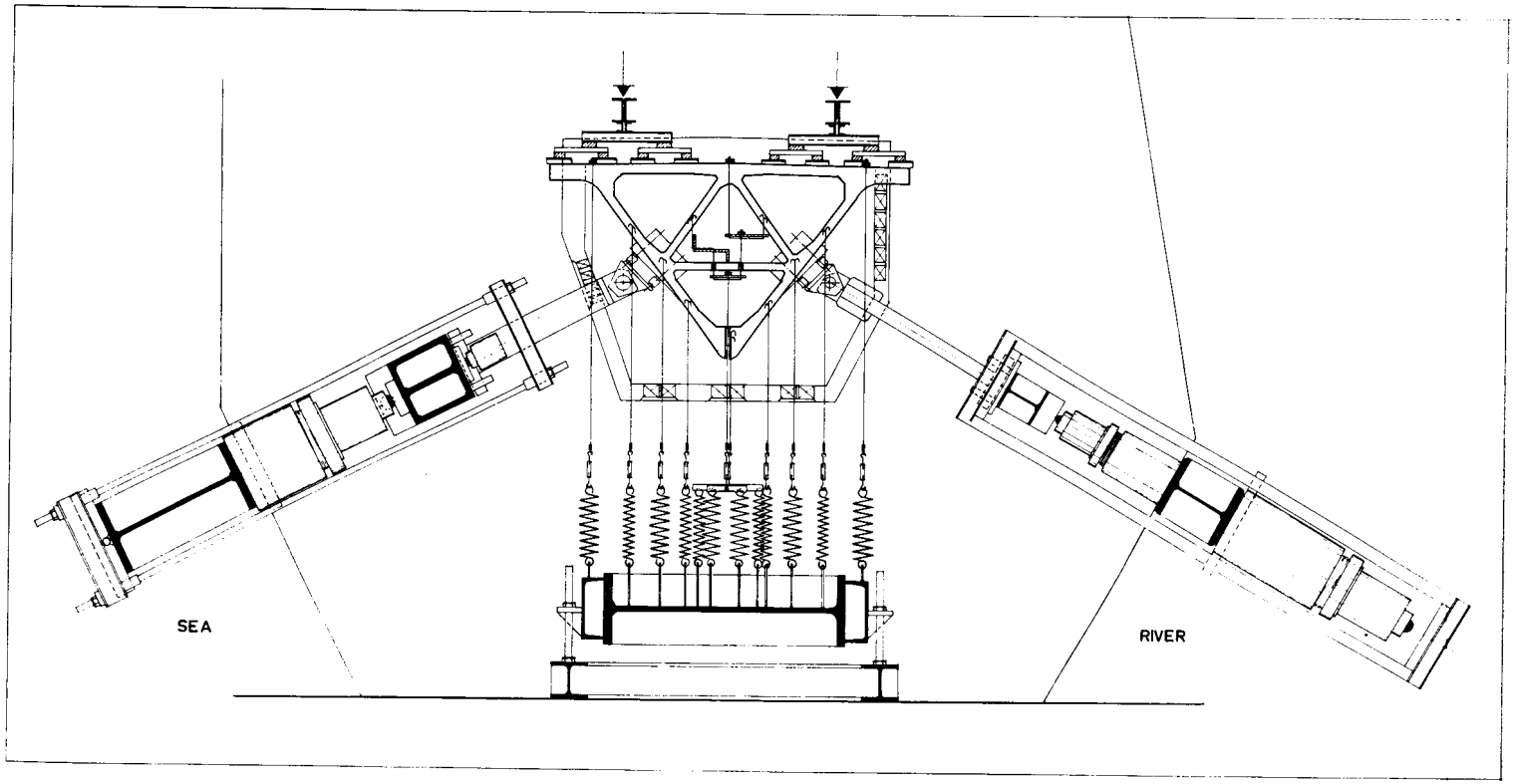

Figure 24. Load distribution in the 1 : 15 scale model

The model was built in exactly the same way as the real girder; precast units were used which were assembled with joints cast in situ. The mild-steel reinforcement in the joints was made continuous.

To verify the calculated stress distribution, the strain on both the external and the internal surfaces was measured with about 700 electrical resistance strain gauges and with mechanical extensometers.

Vertical and horizontal displacement was measured with dial gauges. Periscopes were used to inspect the interior of the girder.

A large number of load combinations were applied to the model, both at the basic load stage (i.e. within the elastic limit) and during overloading corresponding to a load factor of 1.3 (i.e. at the commencement of cracking).

Finally, the compressive load acting from the direction of the sea was increased to 3.9 times the basic load. Testing was then stopped because the strength of the loading rig precluded any further increase.

Some of the results are given in Figures 25 and 26.

Figure 25 shows the distribution of the direct stress in the central cross-section for a compressive load of 220 tons per linear metre from the direction of the sea and a live load of 0.55 ton per sq. m.

Fair agreement was found between the measured stresses and the values calculated in accordance with the beam theory.

Figure 26 shows the compressive zone deduced from the measurements for the load combination made up of the weight of the structure itself, prestressing and a threefold compressive load acting from the direction of the sea.

The first crack appeared at the junction between the precast unit and the joint at the centre of the span at zero stress. At the adjacent joints checking occurred at a bond stress of 10-20 kg per sq.cm. The joint concrete hardly adhered to the pre-fabricated Nabla section at all. The only cracks occurring under maximum load were flexural; no shear cracks had as yet appeared.

The ultimate load was calculated by Mörsch's method; the theoretical figure was not very much higher than the maximum load applied.

5. Research on the concrete

A series of investigations had to be carried out to get a type of concrete that was watertight, would resist the aggressive sea atmosphere and possess minimum shrinkage; it was necessary to enable a decision to be reached on the aggregate to be used (i.e. sand and gravel).

A special blast furnace cement with a higher percentage of granulated slags than usual (i.e. up to 70%) and a lowheat Portland cement part was used for the huge

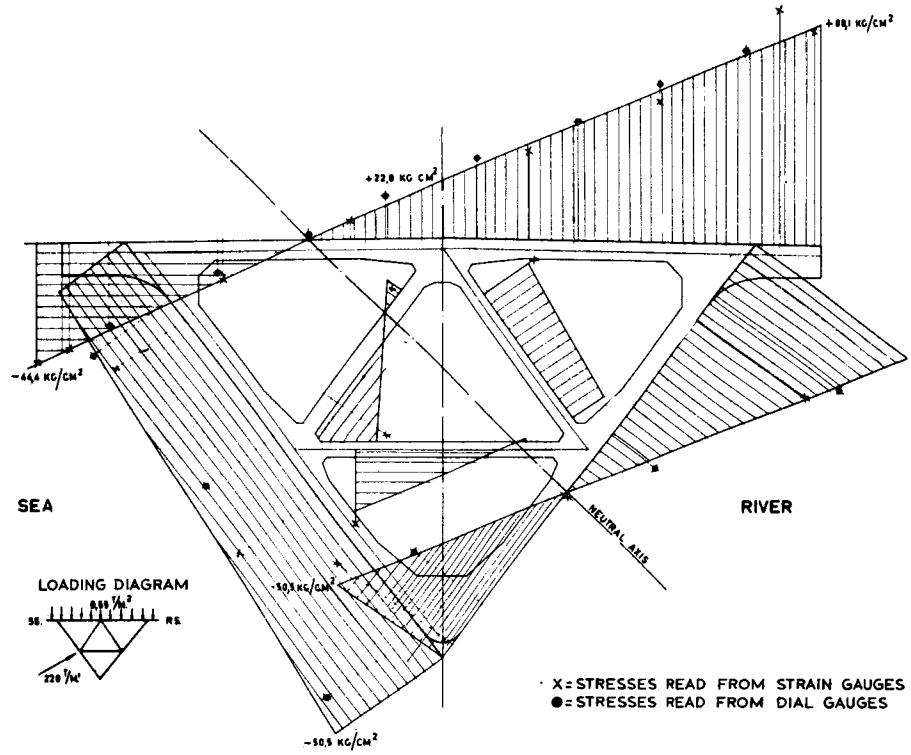

Figure 25. Normal stress distribution in centre section

volume of concrete required for the piers. 300 kg blast furnace cement per cub. m. concrete was used and the water/cement ratio was 0.47.

The mixture of sand and gravel was brought as near as possible to the Fuller curve and an air entraining agent was used to increase the workability.

No cooling pipes were used.

Conventional blast furnace cement with an air entraining agent was used for the concrete of the precast Nabla girder units. 375 kg cement was used per cub. m. concrete and water and cement in the proportion 0.42 : 1 was mixed with the same sand and gravel mixture as was used for the piers.

Crushed materials were not required. After casting the units were slowly heated to 45 °C. with wet steam, the operation taking 5 hours. This temperature was maintained for another 5 hours, when the steam supply was stopped and the units were allowed to cool in about 6 hours to atmospheric temperature in a shed where they were protected from the wind and other atmospheric influences. The Nabla girder joints

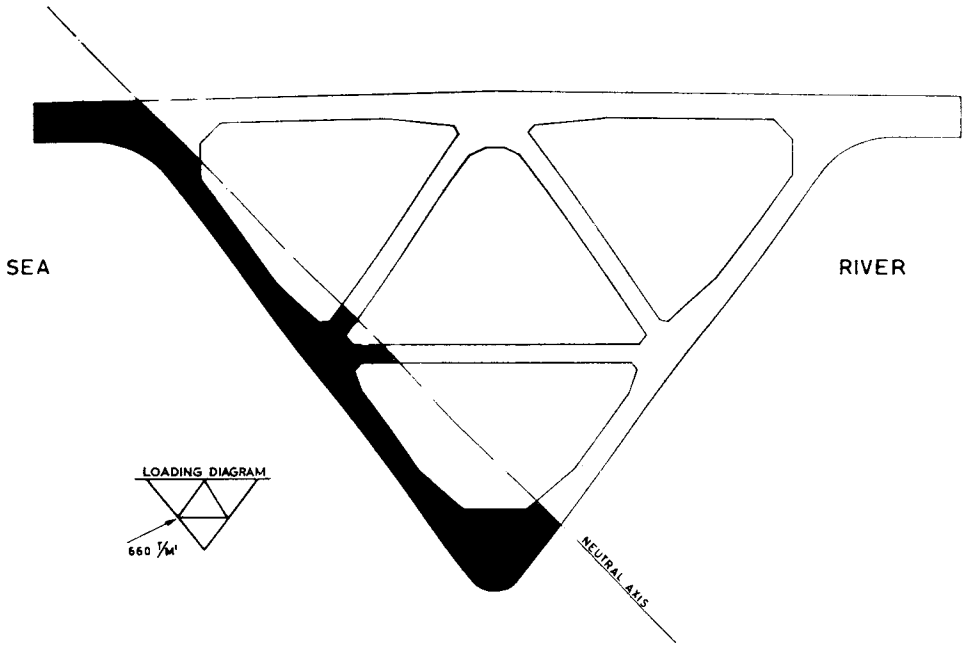

Figure 26. Normal stress distribution in centre section

were made of a concrete consisting of 340 kg blast furnace cement, pozzolith without calcium chloride, a water/cement ratio of 0.42 : 1 and a mixture of sand and gravel near the Fuller curve.

Part of the prestress (i.e. a few kg per sq. cm.) was applied as soon as possible after casting to take up much of the shrinkage and creep.

The cube strength of the "mass" concrete was about 300 kg per sq. cm. after 28 days.

The cube strength of the concrete used for both the precast units and the joint concrete was over 400 kg per sq. cm. after 28 days.

100 kg Portland cement, 20 kg Trass and 50 litres water was used for the cable duct grouting.

Experiments were carried out with a view to grouting in winter and preventing the ducts from freezing, but it was clear that the grouting schedule would have to be such as to make it unnecessary to grout such a large number of ducts in winter.

During cold spells in the winter three shifts worked day and night blowing compressed air through the cable ducts to keep them dry and to prevent the concrete from freezing.

The concrete structure was started in 1958 and completed in 1965.

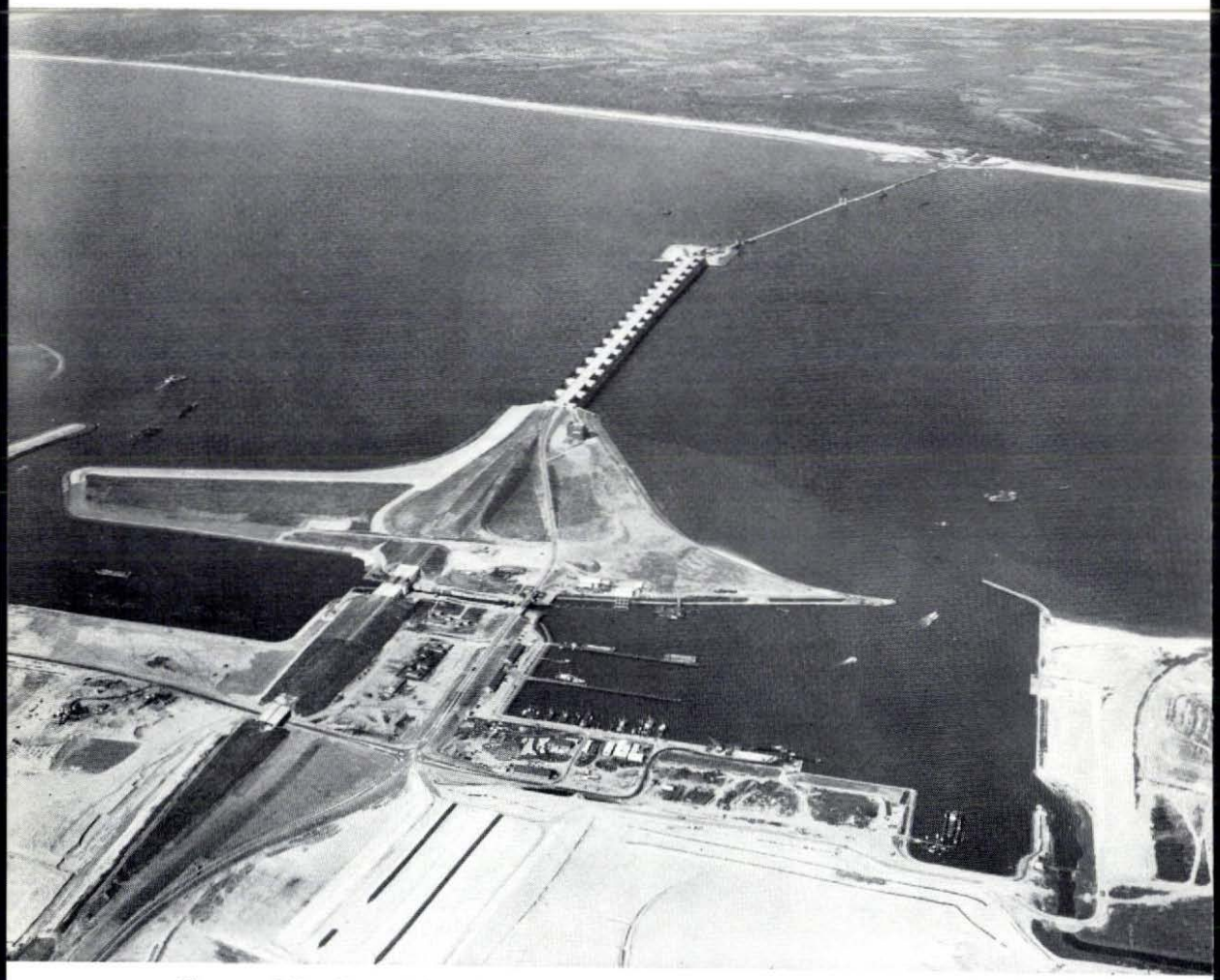

Photograph 3. General view of the sluice-gate complex in the closed Haringvliet with the sea on the left. In the foreground the locks for navigation and fishery (photo Bart Hofmeester)

III. The electro-hydraulically operated segmental gates

1. Introduction

The general plan of the sluice gates in the Haringvliet and the construction and building of the basic structure with "Nabla" beams, etc. are extensively described in the preceding sections.

This section deals with the steel gates, the hydraulic mechanism used to operate them and the electrical installation with its own diesel powered generating station.

2. The segmental gates

An overall impression of the complex and the cross-sections of gates and Nabla beam are again reproduced in Figures 27 and 28 respectively.

The outlets are all 56.5 metres wide; the gates on the seaward side are 8.5 m and those on the landward side 10.5 m high.

As each of the 17 openings has an outer and an inner gate, there are 34 segmental gates in all.

Both the outer and the inner gates are attached to the Nabla beam by four hinged arms; because of the segmental shape of the outer faces of the gates the normal, water-engendered vectors all pass through the centre of rotation, so no load is placed on the lifting mechanism.

As regards the *safety* of the barrier, each gate can wholly replace its partner, although when there is a high storm tide, water may spill over the lower outer gate and run into the basin behind the sluice gates if the inner gate is raised.

Because of its unfavourable forward-leaning attitude the seaward gate has to withstand very heavy buffeting; at 3 m. above A.O.D. the stress due to wave buffeting may mount to as much as 100 tons per running metre and even to very much higher figures in places.

A "pocket" going down to 12 m below A.O.D. had to be incorporated in the structure on the seaward side to cushion the impact of the surging masses of water. Without this, the pressure on the lower part of the gate would be many times greater.

This expedient was resorted to after model tests in the wind flumes at Delft and in the Hydraulics Laboratory at De Voorst in the North East Polder had been completed, while extensive research on the dynamic behaviour of the whole complex of sub-structure, Nabla beam and steel gates revealed that an impact coefficient of 1.35 would have to be adopted for the gate.

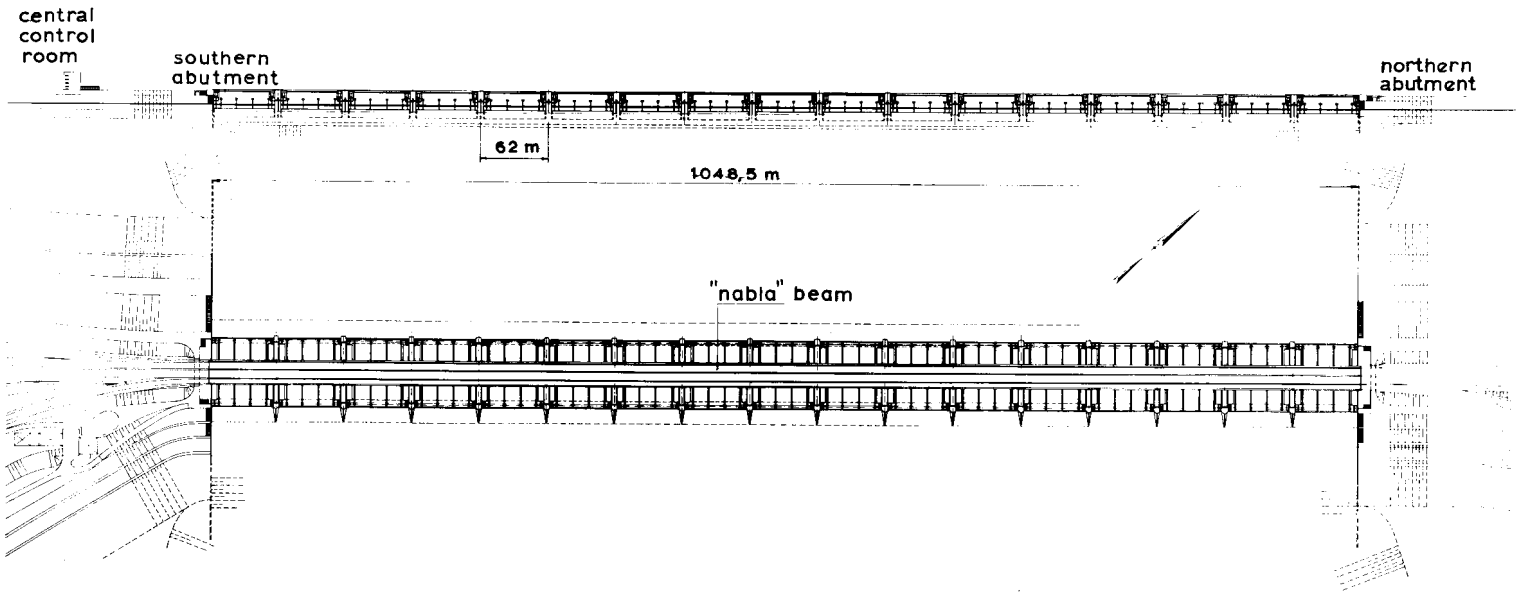

Figure 27. Plan (View from river)

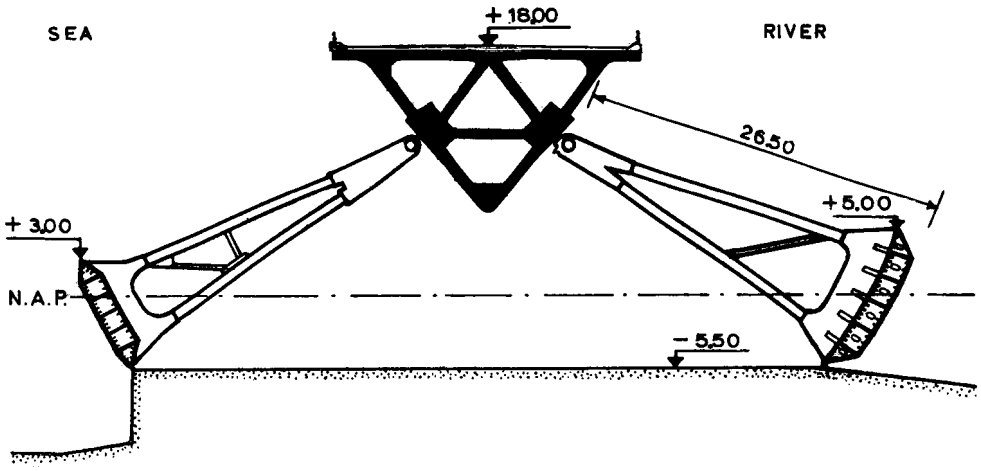

Figure 28. Cross-section of gates and Nabla beam

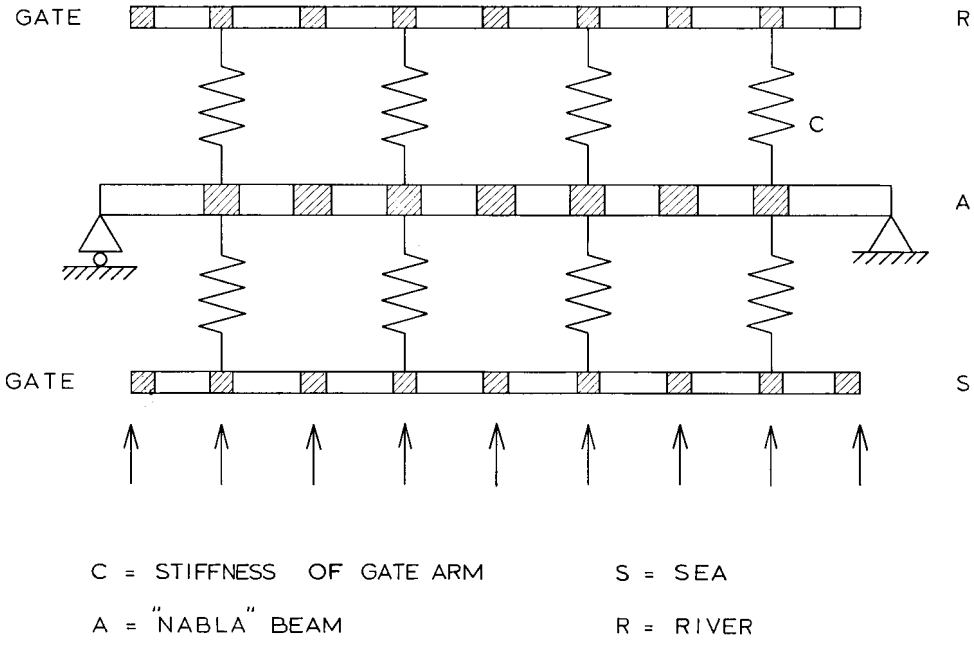

Figure 29. Mass resilience of gates and Nabla beam

The calculations also showed that the impact coefficient for rotation points and the Nabla beam would have to be put at 2.2 in view of the difference between the mass of the gates and the mass of the concrete structure.

The "mass-spring" system used in this research is shown diagrammatically in Figure 29. The mass of both the Nabla beam and the gates is regarded as being concentrated at a number of points. The Nabla beam is supported at both ends; wave buffeting may cause the whole system to vibrate through the "sprung" arms.

At high water levels the seaward gate will not be capable of holding back all the water; should it be impossible to put the inner gate into operation, the outer gate would in any case act as a breakwater and the overflowing water would not do much harm; besides, the contingency would be exceptional.

It was quite safe to design the inner gate to reach 5 metres above A.O.D., for even during the most violent north-westerly storms the impact of the waves can considerably be reduced thanks to the special shape of the side facing the sea.

It stands to reason that the various figures obtained from small-scale model tests cannot be used indiscriminately for the stresses, vibrations, etc. set up in the prototype. Careful study of the scale laws was essential; the readings taken on the site of the completed structure will enable interesting comparisons to be made with the results of the model tests.

The construction itself is undoubtedly sufficiently strong because such factors as the various wave foundations that may occur, the area struck by the waves and dynamic factors have all been estimated on the pessimistic side.

Nevertheless, certain strict instructions for operating the gates that were contemplated when the sluices were being designed may be modified on the grounds of the

Figure 30. Measuring points on gates

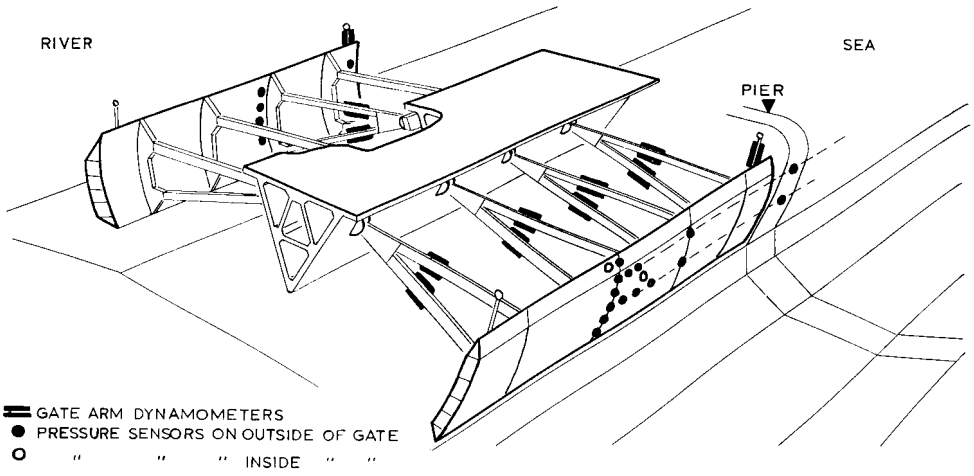

figures obtained in practice, so that those operating the gates will have greater freedom of action.

A number of readings are therefore to be taken in one aperture when the gates are being subjected to various stresses. The measuring instruments shown in Figure 30 will be installed by IWECO-TNO for the purpose.

The figures obtained will no doubt also be useful for similar projects in the future, partly because greater knowledge of wave phenomena will provide a better basis for later model tests.

Other tests besides the model tests referred to above were needed to determine the shape and structure of the gates.

Exhaustive research to discover what materials should be used was of primary importance because the gates would be subjected to very heavy dynamic stresses in an aggressive sea-water atmosphere.

It was therefore decided to use fine-grained SM steel Fe 52 tempered with Al and Si which had to meet the following requirements, both longitudinally and transversely:

σ tensile stress — 52-62 kg per sq. cm.
σ yield stress $\geqslant$ 36 kg per sq. cm.
δ 5 $\geqslant$ 20%
Notch toughness (type 3) at — 20 °C.:
average 6 kg per sq. cm.
minimum 3 kg per sq. cm.
ditto after artificial aging (at — 20 °C.):
60% of the values obtained without aging.

The latter requirement can in fact only be met if the transition-temperature in the notch-bar impact tests without aging is very low because it rises quite considerably after artificial aging.

At the TNO Metal Research Institute a large number of fatigue tests were carried out on the various kinds of steel that would be employed in order to determine the best welding electrode.

Later research revealed that practicable results were also obtainable with an automatic welding method.

After these tests the effect of *corrosion* on the fatigue strength of the welded material had to be investigated. This was done in the Stevin Laboratory at Delft; bending tests were carried out on a large number of welded test beams: dry beams, beams immersed in seawater and beams sprayed with seawater during the test.

The latter two kinds broke at very much lower stresses than those tested dry, so, as was expected, corrosion greatly affected their strength.

The remarkable thing was that the strength of the sprayed beams with obviously corroded surfaces was not less than that of the immersed beams, although the surfaces of the latter were hardly corroded at all.

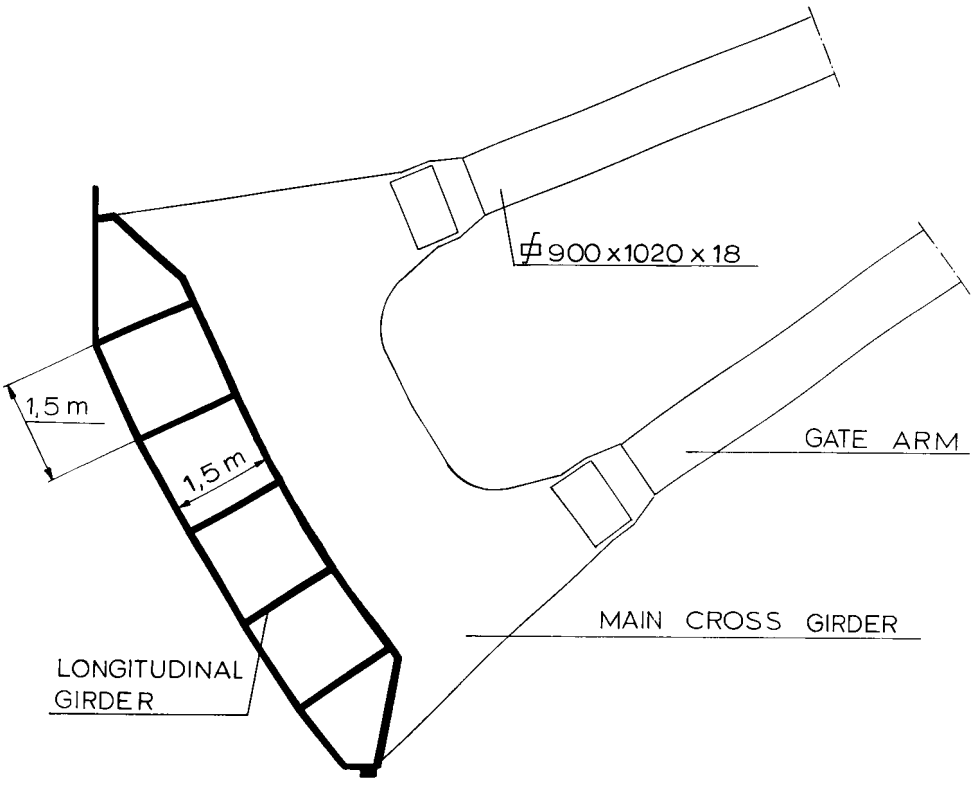

Figure 31. Cross-section of sea gate

The tests also showed clearly that fillet welds had more influence from notches and were more likely to corrode in the groove than K-welds; the former were therefore not employed for the gates at all.

Effective protection against seawater is generally essential to prevent corrosion fatigue. It is in fact quite certain that the combined effect of fatigue and corrosion is synergistic, i.e. their total effect is greater than the sum of the two effects taken independently.

The tests finally showed that preservation with a combination of "epikote" zinc, "epikote" aluminium and "epikote" tar produces the best results. It should be applied in coatings averaging 50, 30 and 220 μm thick respectively. The sheds built for the preservation work to be carried out on the assembly site were large enough to accommodate half a gate at a time. It was thus possible to meet the requirements of a minimum temperature of 10 °C. and a relative humidity below 60%.

In addition, the gates were given cathodic protection by placing aluminium anodes inside the gate and applying an electric current to the outer walls.

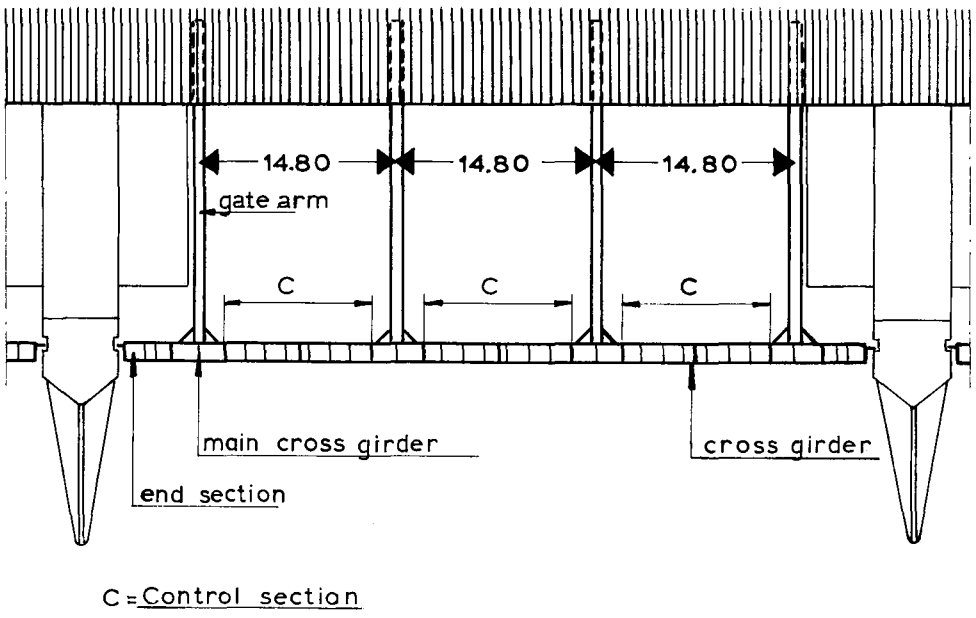

Figure 32. Horizontal section of gate

After these introductory remarks on stress, the selection of materials, etc., we can now deal with the construction of the steel gates.

In cross-section, the front of the gate has a double wall divided into compartments by a number of horizontally placed transverse girders (Figure 31). The surface must be smooth so as to prevent excessive resistance when lifting the gates through ice floes.

Longitudinally, each gate consists of three central sections, each nearly 15 m long and two end sections, each about 7 m long (Figure 32). Double main transverse girders to which the arms are attached are fitted between each of the five sections. The four arms transmit the heavy dynamic loads to the concrete Nabla beam.

The front and back walls of the compartments are made up of orthotropic plates with transverse ribs of flat steel and inverted tee-sections as cross members. At five points in each section the shafts are also stiffened with trusses. Most of the plates are between 10 and 12 mm thick; only near the main transverse girders is the thickness of the longitudinal bars increased to 30 mm.

As observed in the paragraph on the testing of materials, there are no fillet welds; the joints consist of V, X and K seams. The horizontal girders are provided with a large number of triangular holes to allow water to flow in and out when the gates are moved; only near the arms are there a few air chambers; the other compartments are in open communication with the water.

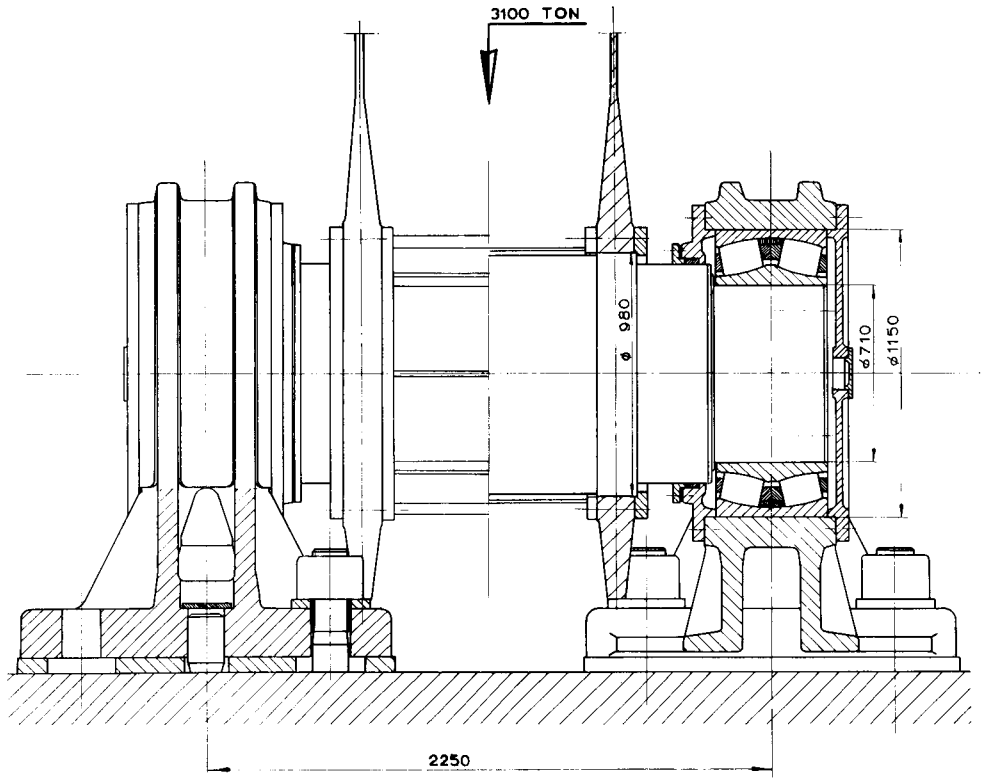

Figure 33. Pivot of sea gate

Needless to say, the holes upset the pattern of the dynamic loads. The most suitable shape of hole was determined by means of photo-elasticity tests.

The arms, too, consist of hollow sections attached to the double-walled main transverse girders with strong tie plates.

The pivot points on the Nabla beam consist of two heavy eye plates (rolled plates 160 and 210 mm thick), in which the pivots are mounted (Figure 33). The pivots (largest diameter 980 mm) are forged from vacuum steell and those on the seaward side weigh about 12 tons each. The highest stress per pivot under extreme conditions may be about 3,100 tons.

The inner rings of the large roller bearings are mounted on the pivots on both sides of the gate arms; their outer rings (max. diameter 1,150 mm) are housed in cast steel bearing housings. The chairs are attached to the Nabla beam with heavy prestressed bolts 150 mm in diameter. A number of the large bearings required for the project are pictured in Figure 34 (680 of these huge bearings have been ordered).

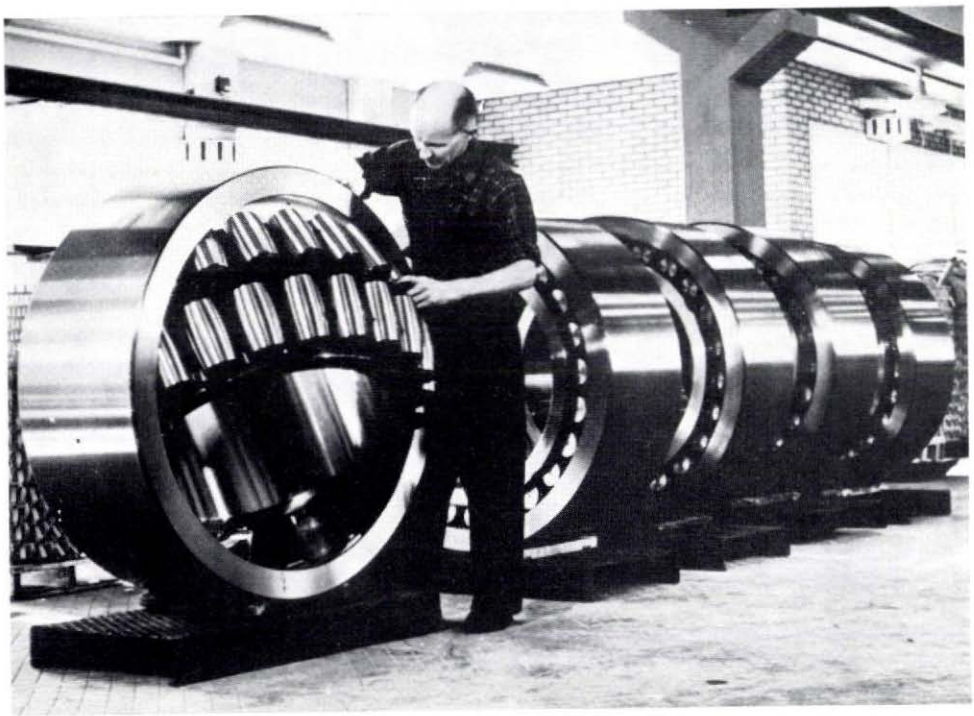

Figure 34. Some of the roller bearings for gate pivots (photo S.K.F.-Netherlands)

The Haringvliet is not only being dammed off because it will form a safe barrier against high storm tides but also because it will help to maintain a fresh-water reservoir on the landward side. It is important for both agriculture and horticulture in this part of the country that the soil salinity be kept as low as possible. Much attention has therefore been given to achieving an effective seal when the gates are closed. When closed, the gates rest on a hollow rubber strip fitted to the concrete sill and there are inflatable rubber tubes along the edges (Figures 35 and 36). Inflatable tubes are necessary because the profile of concrete piers made on the site cannot be expected to conform exactly to that of the ends of gates manufactured in construction workshops (slight differences in measurements can be eliminated by using inflatable rubber tubes); besides, changes in temperature may cause the gates to expand or contract.

As the rubber tubes cannot absorb the forces of wind and waves acting on the gates in a longitudinal direction, the sides of the gates have been provided with guides running on two resilient buffers on each pier.

Figures 37 and 38 show the gates being made in the works. The component parts were manufactured in batches in eight different workshops and assembled in two different places. Consequently, the tolerances had to be very closely adhered to by the

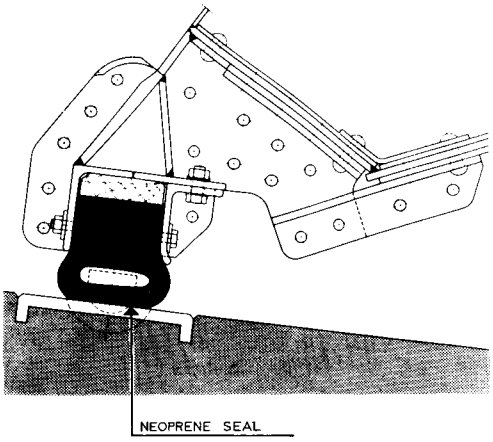

Figure 35. Seating of river gate

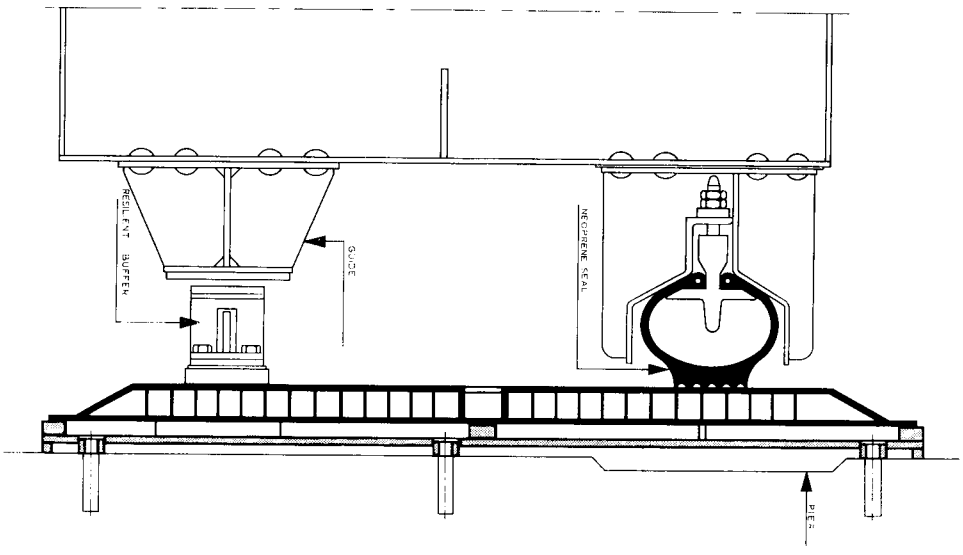

Figure 36. Horizontal section of gate with seal

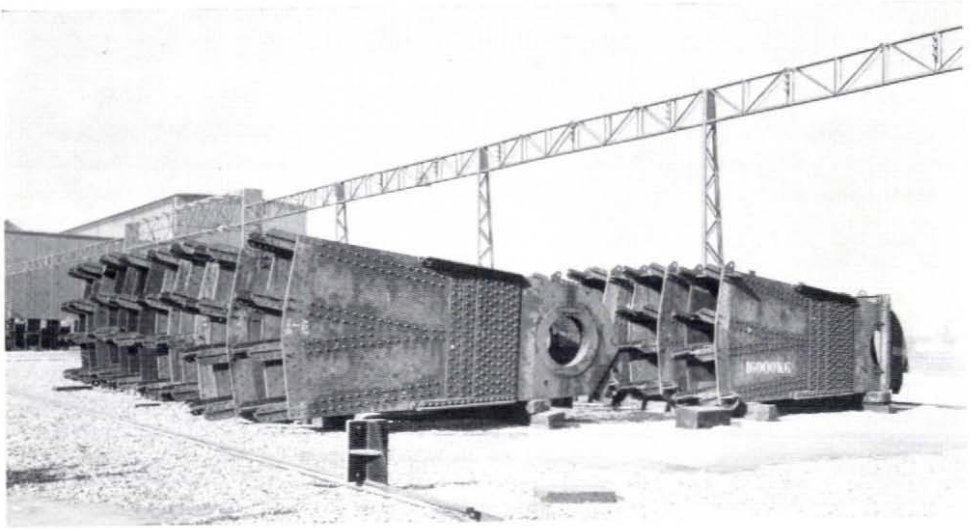

Figure 37. Pivot-ends of gate arms under construction

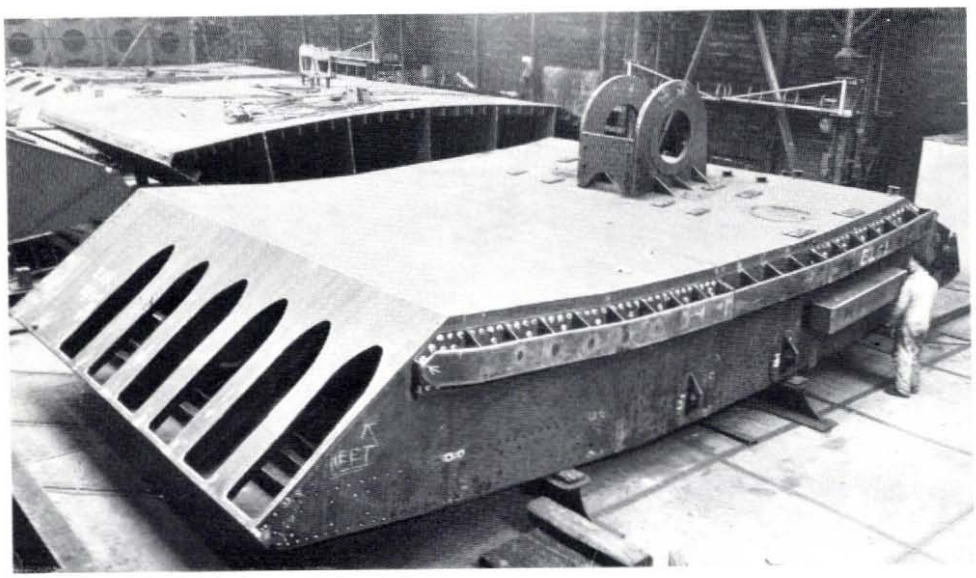

Figure 38. End section of gate in workshop (with eyes for suspension arm)

Figure 39. Nestum crane. In the foreground the duct (see arrow) for the electricity cables between control room and southern abutment

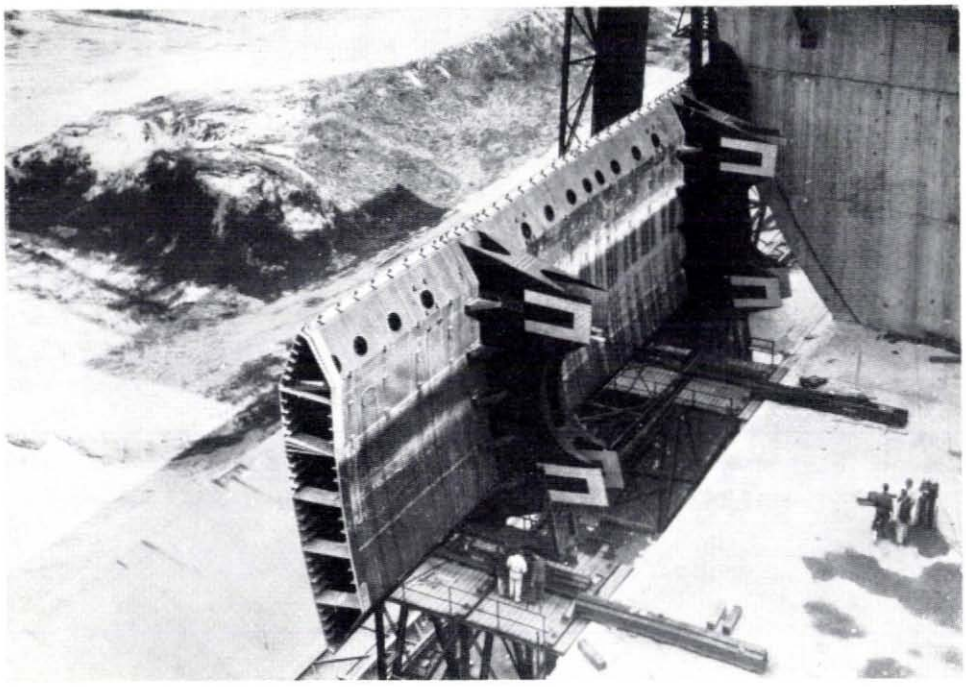

Figure 40. Assembling half of gate

various firms that made the components; they were practically rigid when they reached the assembly stage, so it would have been hardly possible to correct any errors. To achieve the required accuracy the various components were placed on heavy jigs and welded together. After welding, the measurements of each piece could be checked with a very accurate jig.

As already stated, the components manufactured in this way were conveyed to two assembly points, one in Utrecht and one in Rotterdam, where they were joined to form bigger units.

At this stage the large holes in the four arms were bored to receive the pivots; after anti-corrosion treatment the pivots with their bearings and bearing housings were fitted. Two half gates and the loose arms were then ready to be transported to the Haringvliet site. They were placed on special platforms; half a gate weighs about 200 tons. They were unloaded onto specially built bogies that ran on a double track from a jetty that moved up and down with the tides and moved to the concrete floor of the sluice near the Nabla beam.

The "Nestum" crane (Figure 39), which was also used for the fixed structure, then moved the parts of the gates to the appropriate seaward and landward side of the sluice openings. The gates were then completed on the spot (Figure 40).

3. The hydraulic lifting gear

Needless to say, a large number of designs were prepared from which the most suitable mechanism for operating the gates could be selected. It was postulated that the gates should be raised and lowered by machinery placed in the piers and linked to either end of each gate. As the ends are 60 metres apart, the two units operating a single gate could hardly be mechanically interconnected.

One difficulty was that the tests in the Hydraulics Laboratory had not been completed when the initial designs had to be prepared. The engineers were of course already aware that a construction so exposed to the waves would be subjected to heavy stresses, but in reference books little was to be found on the actual magnitude of these forces.

Accordingly, the initial plans for lifting gear were drawn up for gates weighing 275 tons each, whereas later, when more definite data had become available, the weight of the gates had risen to about 500 tons. This of course called for quite a different type of lifting mechanism. One of the first designs is shown in Figure 41; this was a fairly orthodox construction in which the gate was moved up and down by a rack, pinion and gear-box arrangement and an electric motor. Similar variants with cable and chain drives had already been designed, but in all of them a large proportion of the weight of the gate was balanced by a counterweight, so that a much smaller motor could be used (only the preponderant weight of the gate then having to be moved).

However, the tests conducted in the Hydraulics Laboratory showed that particularly in this case the weight of the gate should not be reduced by a counterweight, since during storms with waves of a certain height and periodicity such great upward pressures would be exerted on the horizontal girders that the gate would be lifted up to a fairly great height.

The fact that the gate's own weight would increase as a result of the horizontal wave impact did not in the end turn out to be too serious; reduced though its own weight is by the lift of a few air chambers near the main transverse girders, it is now sufficient to compensate the upward vectors.

Anyway, abandoning the counterweights necessitated drastic alteration of the plans for the operating mechanism; moreover, it was then thought that it would be advisable to give up the idea of having towers at each pier (required for such purposes as housing of the operating mechanism) so that motor traffic over the Nabla beam would not be endangered when passing such structures in strong cross winds.

The operating mechanism design ultimately selected is shown in Figure 42; the hydraulic lifting gear is housed in engine rooms incorporated in the piers. In view of the very heavy stresses that occur, a hydraulic power unit was indeed much to be preferred; the force required to lift half a gate is about 400 tons vertically. About half of this is the gate's own weight; the remainder is mainly due to the waves. It is true that the gates need not be opened during heavy wave onslaught from the west but

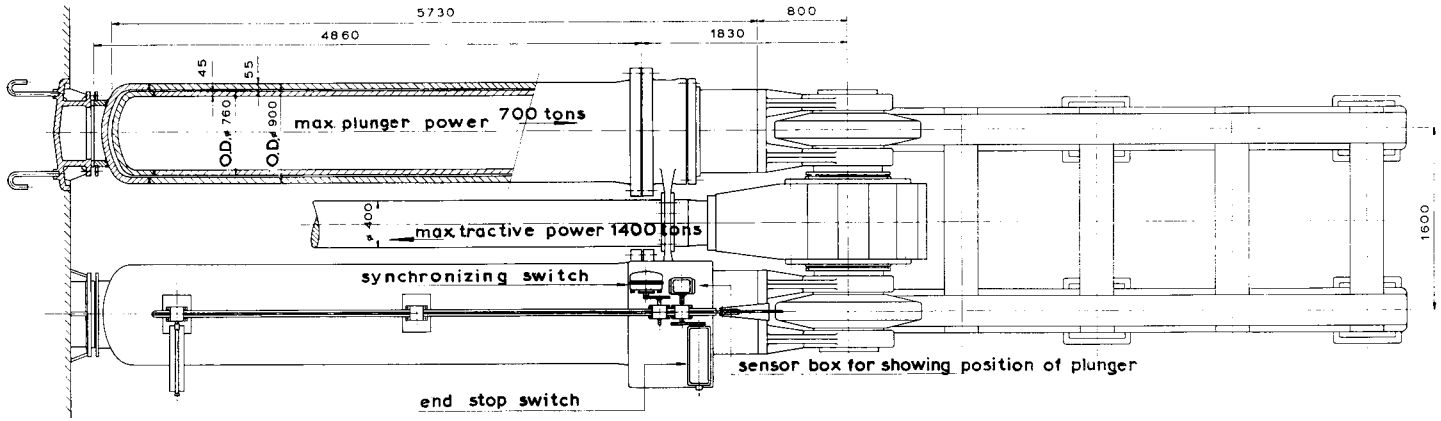

Figure 43. Plan of hydraulic system

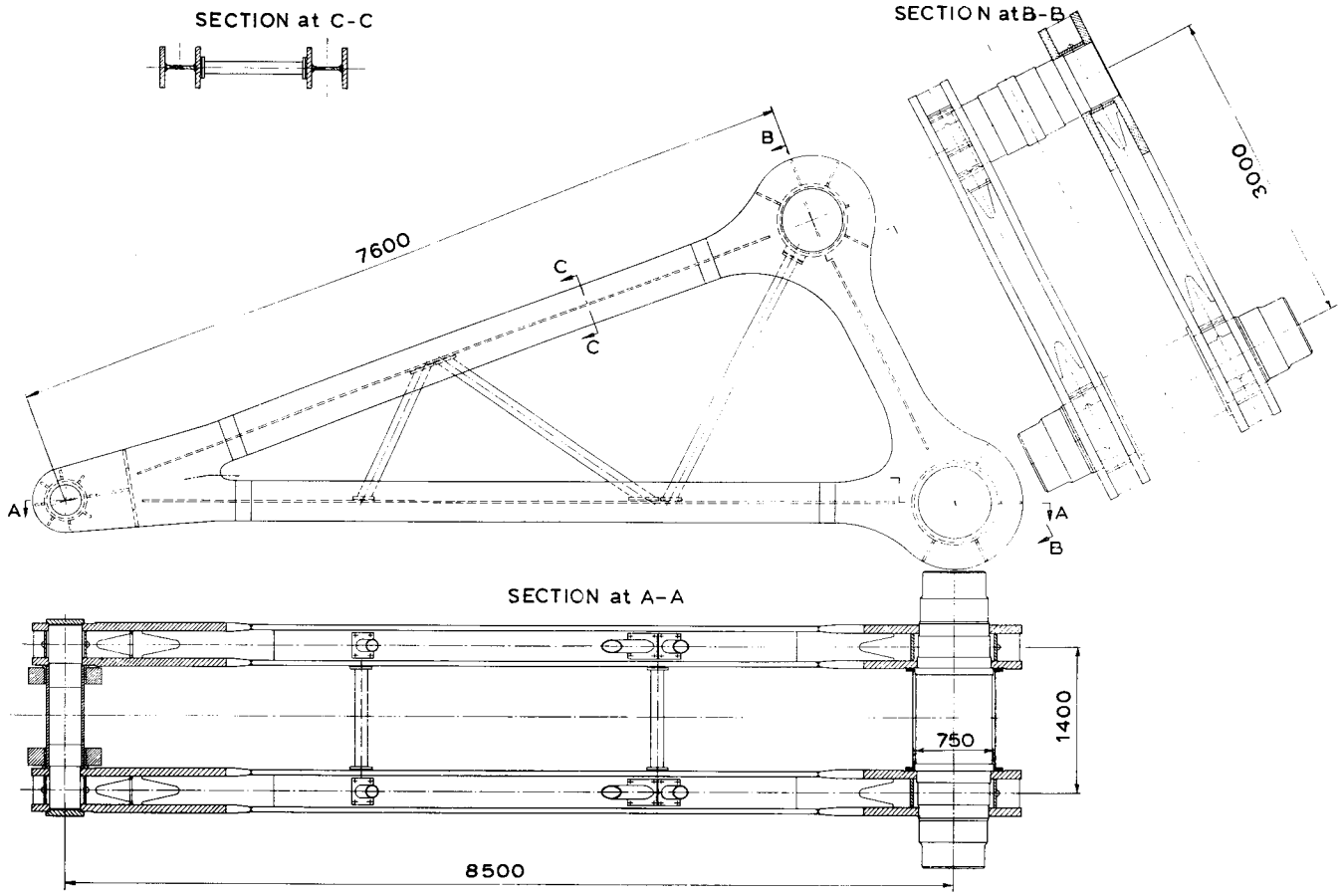

Figure 44. Triangle

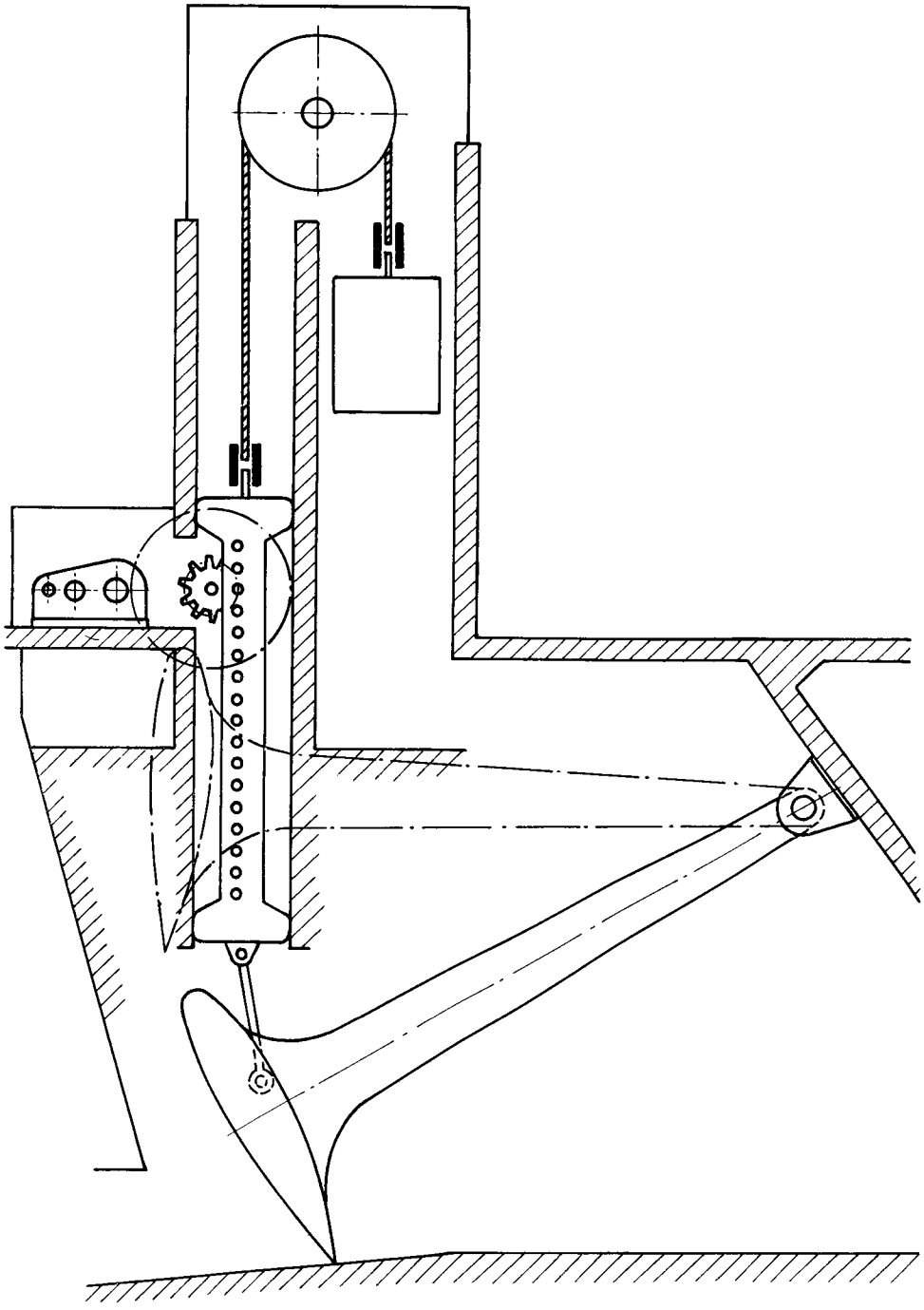

Figure 41. Tentative scheme for mechanism

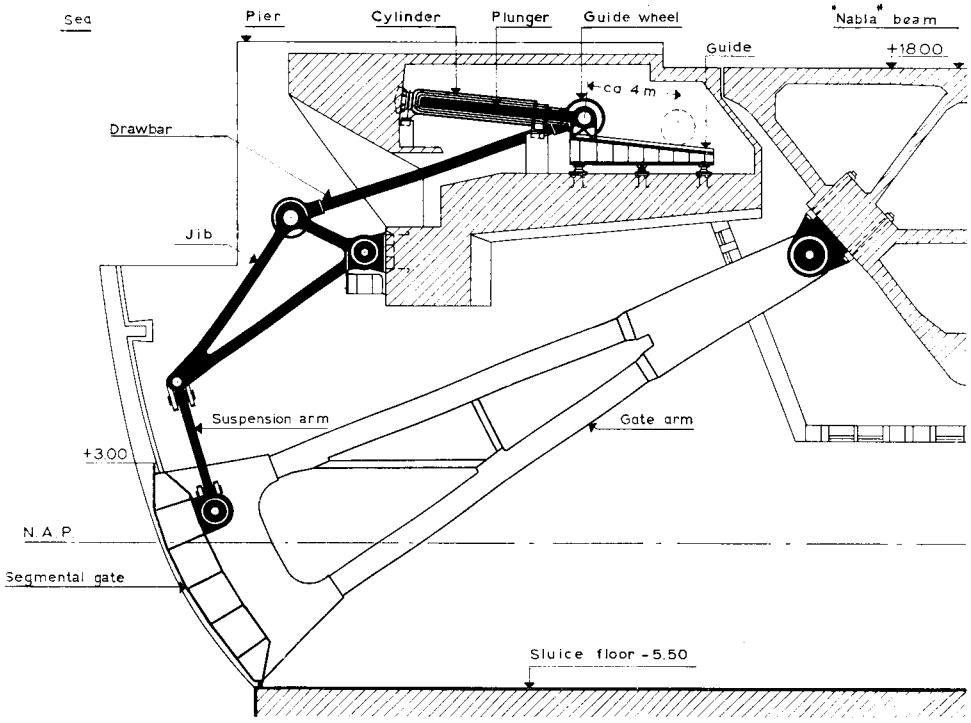

Figure 42. Final form of mechanism

after a long stormy period the water level in the Haringvliet may rise so sharply (partly as a result of the continuous discharge from the rivers) that it may be necessary to open the gates at the first suitable ebb tide to get rid of the surplus. On such occasions, the waves may still be so strong as to put a heavy load on the operating mechanism.

Moreover, considerable intermittent downward stresses will be set up by the masses of water falling down on the gates when the water level is high. Part of the heavy downward stresses will be ascribable to the fact that the water level inside the gate will not be able to follow the wave motion outside it because the holes in the horizontal girders are relatively small (the water has to flow in and out of the gate through the holes in its *under*side). These vertical forces may also be directed *upwards.*

Moreover, the suction set up by water passing across the lower edge of a partly raised gate when excess water is being discharged into the sea will tend to pull the gate down, which is tantamount to increasing its weight; little extra power will be required to overcome this, however.

All these factors combine to produce a total load of 400 tons transmitted to the operating mechanism by a suspension rod at either end of the gate. The mechanism consists of two 90 cm diameter cylinders side by side (at a slight angle); oil is forced into the cylinders by means of pumps, the plungers actuate drawbars and triangles and the gates are lifted.

The total lift is about 11.5 m (i.e. the lower edge of the gate moves from 5.5. m below A.O.D. to 6 m above A.O.D.) and the stroke of the plungers is over 4 metres. This means of course that the power to be delivered by the plungers will be considerably in excess of the load placed on the gate.

The gate rotates through 30° as it passes from its closed to its fully opened position and the triangles sweep through roughly 90°; the transmission ratio between the vertical rod attached to the gate and the plungers is therefore not constant as the gates are raised or lowered. When the load on the suspension rod is less than 400 tons, the force exerted on the plungers may be as much as 1,400 tons. Such a heavy load is best taken by two cylinders, a single cross head linking the two plunger rods (see Figure 43). By making the boom double walled and the suspension rod to the gate single, there are many suitable ways of making the connections.

The construction of the triangles is shown in Figure 44. The long rods are made up of vertically placed 50 mm thick flanges and 25 mm body plates, and the flanges for the short leg and at the corners thicken to 80 mm. Going by photo-elasticity analysis (Figure 45) a steel was selected similar to that used for the gates (Fe 52), for these parts, too, are subjected to heavy fatigue strain. When a gate is partly raised, the flow underneath it may cause it to vibrate; this will happen virtually independently of the water level and aperture and the vibration will occur at the operating mechanism's natural frequency. The intermittent forces exerted by the masses of water falling down on the structure will also cause vibration when the waves are pounding the gates. Accordingly, millions of stress changes may occur in the structure during its life time (in a frequency of 1.5 to 2 Hz.).

The welding together of the very heavy plates was most carefully executed to prevent dangerous notch working. Moreover, all the welds were x-rayed afterwards. The plates were pre-heated before being flame cut and welded and the whole construction was annealed at about 625 °C. Figure 46 shows a triangle during assembly.

The triangle is connected to the hydraulic power unit in the engine room by means of a large drawbar. It is 400 mm in diameter and is threaded at both ends so that it can be screwed into the heavy eye pieces. The eye pieces can rotate on the upper pivot of the triangle and on the cross head linking the plungers, as they are fitted with two roller bearings (outside diameter 920 mm) (see Figure 47).

There are two 1.3 m diam. rollers on the cross head which run on sloping tracks, guiding the plungers as they move outwards. As the drawbar moves at an angle to the plunger rods (the cylinders had to be set at an angle to distribute the tremendous stresses throughout the concrete structure), the load on each wheel may reach about 300

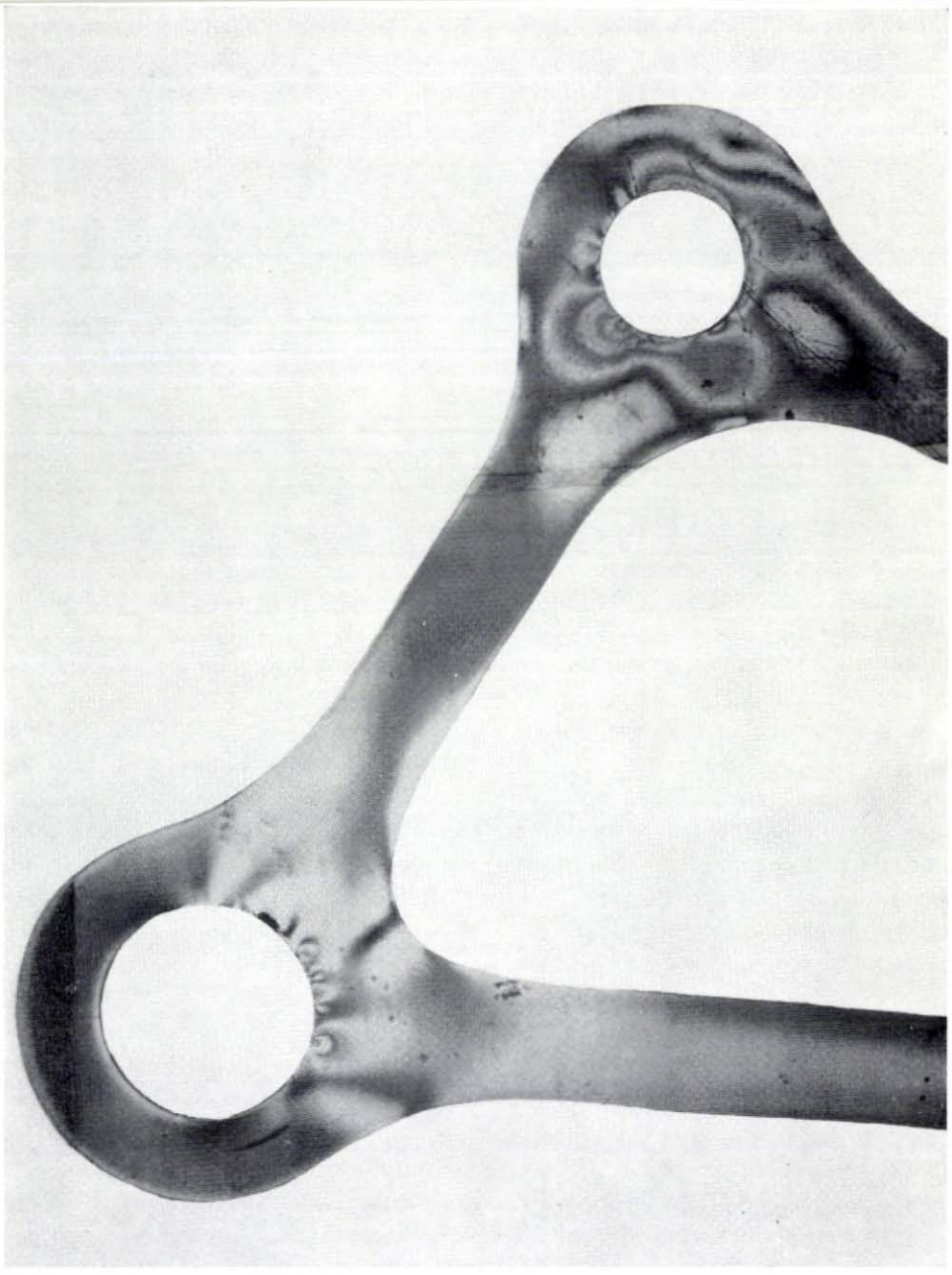

Figure 45. Photo-elasticity test of triangle

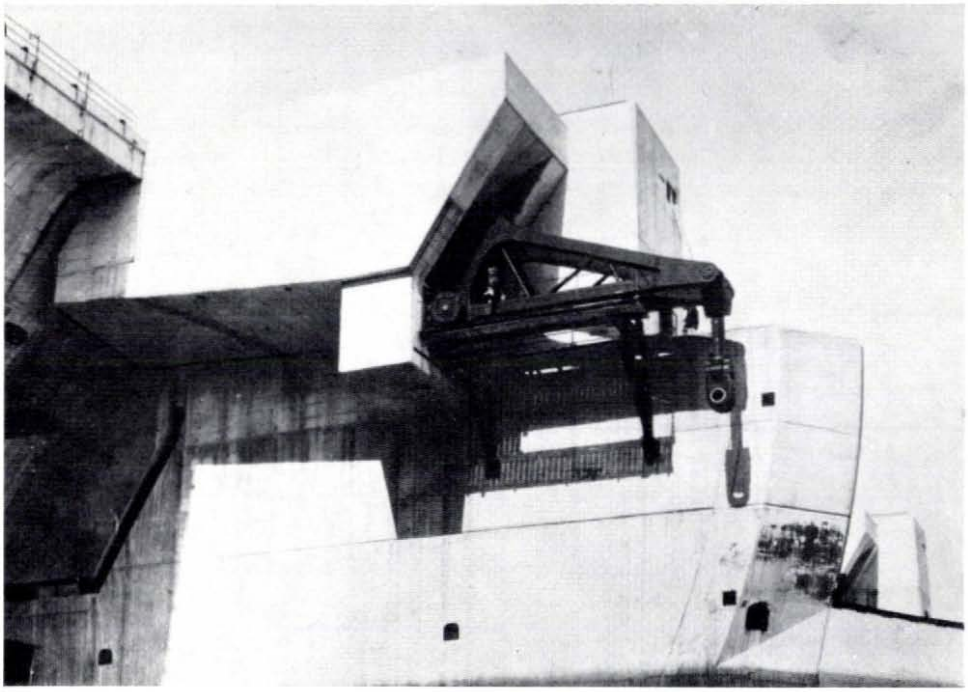

Figure 46. Triangle on assembly platform

tons. To stand up to this, the wheels were made of hardened cast steel; the cast steel tracks are less hard, as it is easier to repair or replace worn tracks than worn wheels.

The plunger rods are guided not only by the wheels but also by bronze bushes in the cast steel structure to which the cylinders are attached with prestressed bolts (Figure 48). The bushes are provided with packing glands with which the plungers are sealed off; the two cylinders are interconnected with coupling plates.

The forces at the back of the cylinder are transmitted direct to the concrete through the cast steel housings encased in concrete. Since, as already stated, vibration may occur when the gates are partly raised to allow excess water to reach the sea, the cylinders and plungers have also been subjected to various tests. The equipment available in the laboratory of the State University at Ghent made it possible to have fatigue tests carried out on a full-size cylinder. Since 136 cylinders and plungers had to be manufactured it was worth trying to find an economical way of constructing them. For this purpose a number of tubular objects and connections of different shapes and sizes were welded to the model to ascertain which execution was the most suitable for standing up to about one million vibrations (with pressures ranging from 40 to 160 atm.).

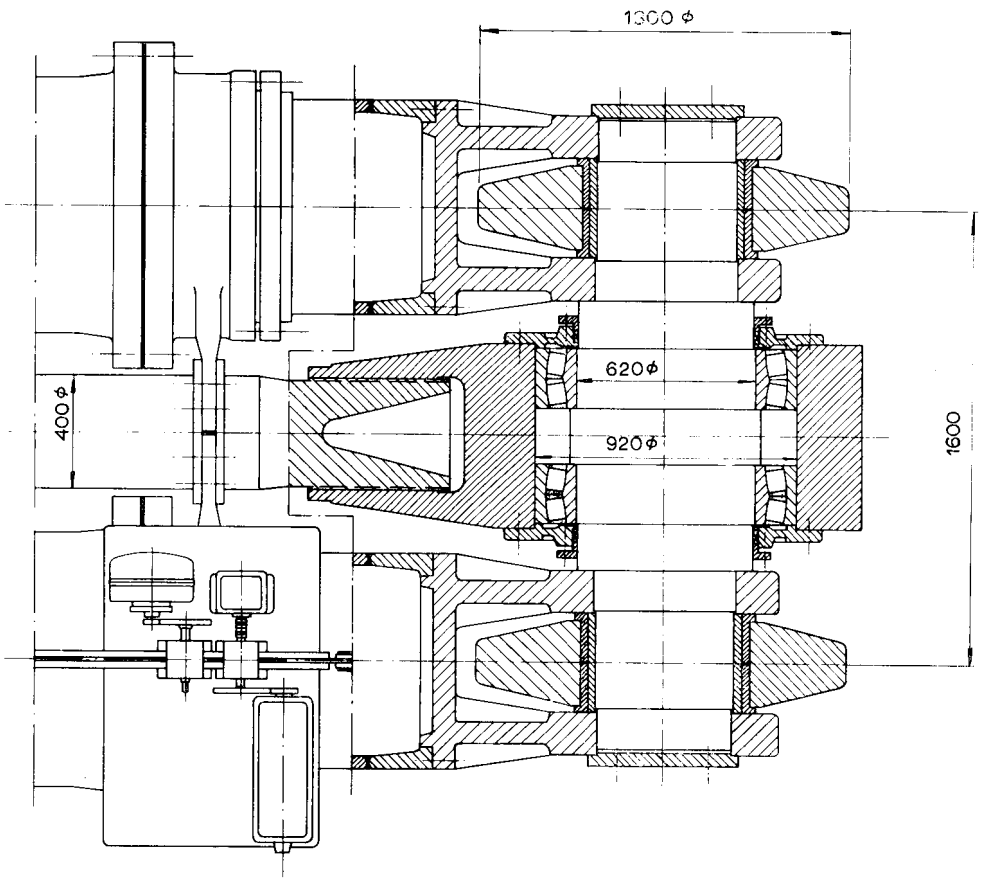

Figure 47. Gudgeon pin linking plunger to drawbar

Under the most adverse circumstances an oil pressure of 150 atm. will be required for moving the gates. This pressure is produced by an axial-flow plunger pump with a constant capacity of about 150 l. per min.; this will move the gate at 1 cm per sec. (measured at the front); it takes about 20 minutes to open or close the gates fully.

The hydraulic circuit is shown in a somewhat simplified form in Figure 49. When the gate is being raised (see Figure 49a), the pump, driven by a 60 H.P. electric motor, feeds oil at the required pressure to the cylinders through one-way valves. The gate is lowered (see Figure 49b) by its own weight: on electrically opening a valve the oil flows back under pressure through the pump to the tank. The power generated by the gate is returned to the power net by means of the asynchronous electric motor; only if the power is generated by the standby diesel engines (see paragraph 4) is the energy absorbed by resistances.

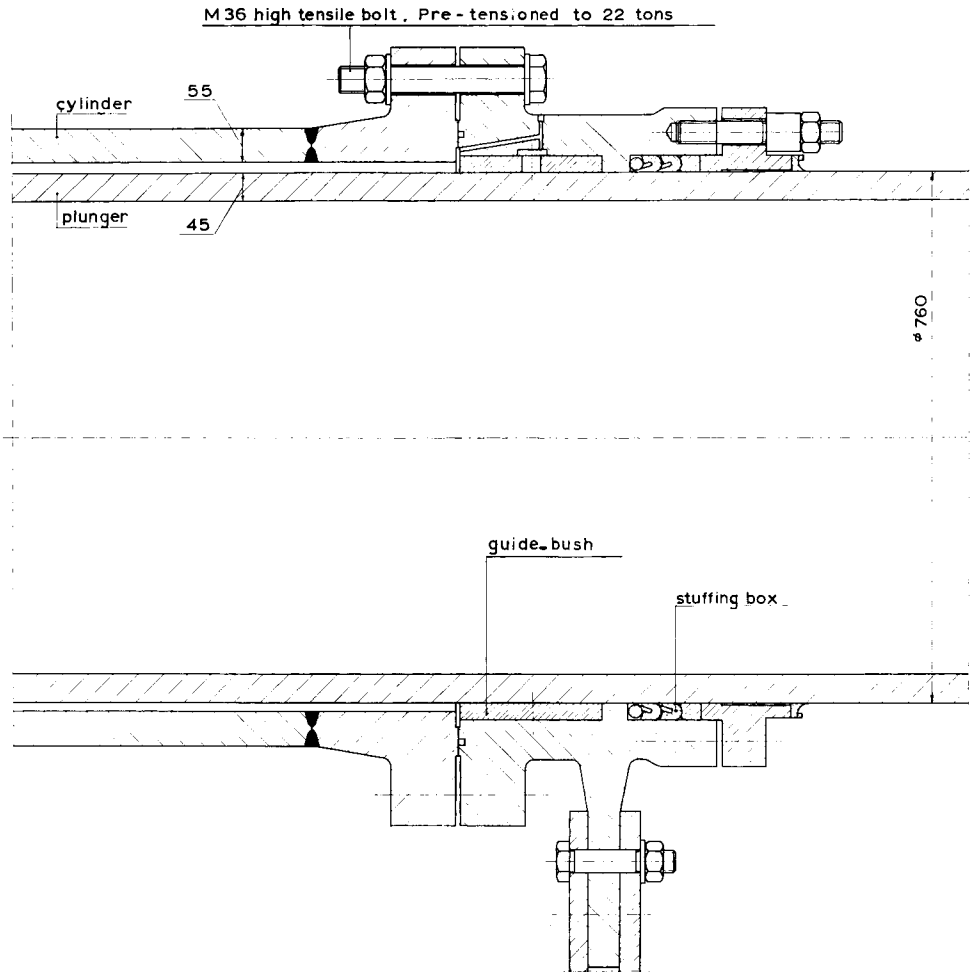

Figure 48. Part of plunger and cylinder

The end stops and the devices that prevent the gate from getting in too crooked a position (the hydraulic forces activating it at both ends being independently generated) are described in the section on the electrical installation.

It should be noted that the steel plunger rods have to be protected from the damp and corrosive air in the engine room, for the gates may have to be kept open for long periods when there is much river water to be discharged. This is done by means of an automatic device by which each plunger is sprayed with a protecting layer of oil during each outward stroke.

To enable the gates to be lifted in the event of a total breakdown of the electrical installation, four mobile emergency units have been purchased, each consisting of a

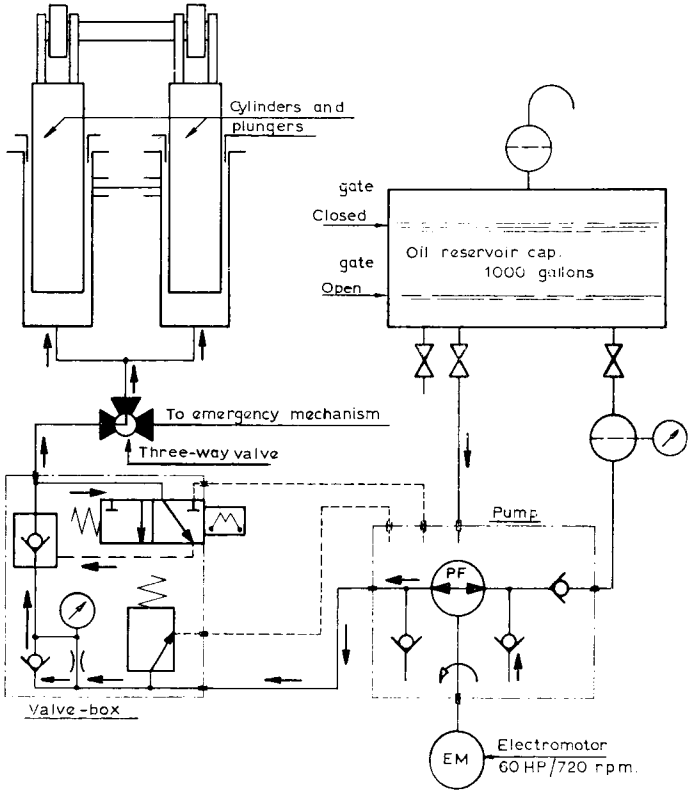

Figure 49a. Diagram showing operation of hydraulic system when raising gate

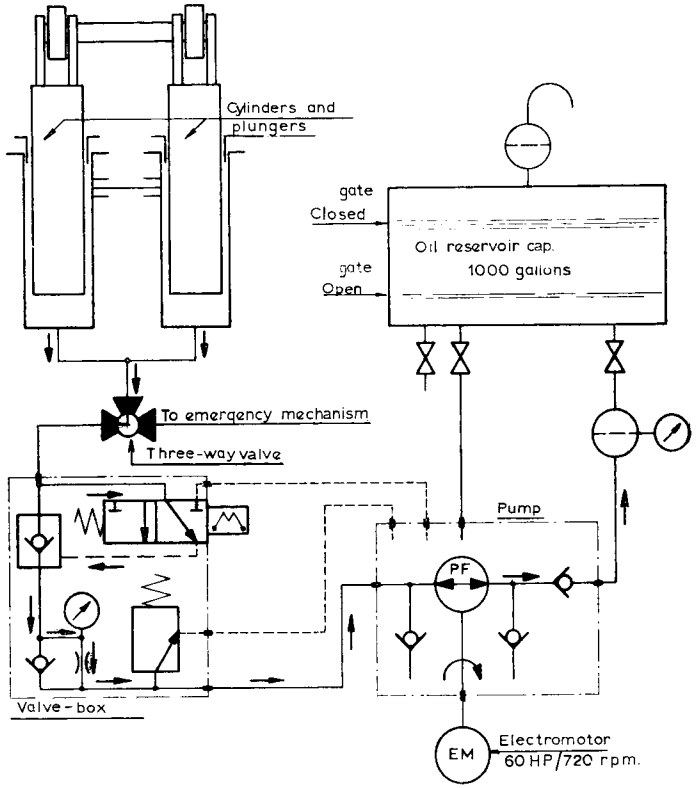

Figure 49b. Diagram showing operation of hydraulic system when lowering gate

petrol engine with its own hydraulic pump. They can be driven over the Nabla beam to the piers where they are needed: the connection points marked in Figure 49 are located in niches at the side of the road. A hydraulic circuit can be obtained by connecting hoses to these points, after which only the parts of the permanent installation that are really indispensable come into action. These emergency units need not be used for lowering the gates: on opening a valve the gate will go down by its own weight, a regulating valve preventing it from going down to quickly.

4. The electrical installation

The pumps of the hydraulic lifting gear are driven by alternating-current motors with special squirrel-cage armatures developing 60 H.P. at 500 Volts. This maximum low-tension voltage was decided upon in order to minimize the voltage drop in the cables. For the same reason the feeder transformers were distributed over the entire length of the sluice-gates: one each at alternate piers that in normal circumstances supplies the current needed for operating the gates in the two adjacent openings.

The transformers are fed from a 10,000 volt ring main. This main begins in the central control room near the southern abutment: current can be generated by the system's own diesel plant there or taken from the high-tension transmission line of the Rotterdam grid system that will be laid after the whole sluice-gate-complex is completed. The entire supply system is shown diagrammatically in Figure 50: the 1,300 KVA generators driven by two 1,500 H.P. diesel engines are on the left. They are large enough to operate all the gates that may have to be lifted under maximum load; in most cases one diesel unit will suffice. For the installation is so designed that only one of the two gates in each aperture can be moved at a time. Therefore current need only be supplied for 17 of the 34 gates at a time (each gate with its two 60 H.P. motors).

Consequently, there is a considerable reserve of power from the combined supply of diesel plant and mains. Similar safeguards are provided in the other parts.

For instance, if a transformer should break down, the circuit can be altered at each pier by means of remote-controlled switches, so that the work of the faulty transformer can be taken over by one of the adjacent ones. A defective section of the high-tension transmission line can also be cut out if necessary.

The diesel units can be controlled at the units themselves or from a switchboard in the adjacent switch room (Figure 51). Each generator can be operated for a short time in parallel with the national grid system, e.g. when switching over from the grid to the diesel units. This obviates the need to interrupt the current. Afterwards the other generator can be put into operation if required.

The operating staff in the control room at the top of the building receives a signal on the large instrument panel when the required voltage has been reached. Figure 52 shows the scale model made for the purpose of designing the various parts of the

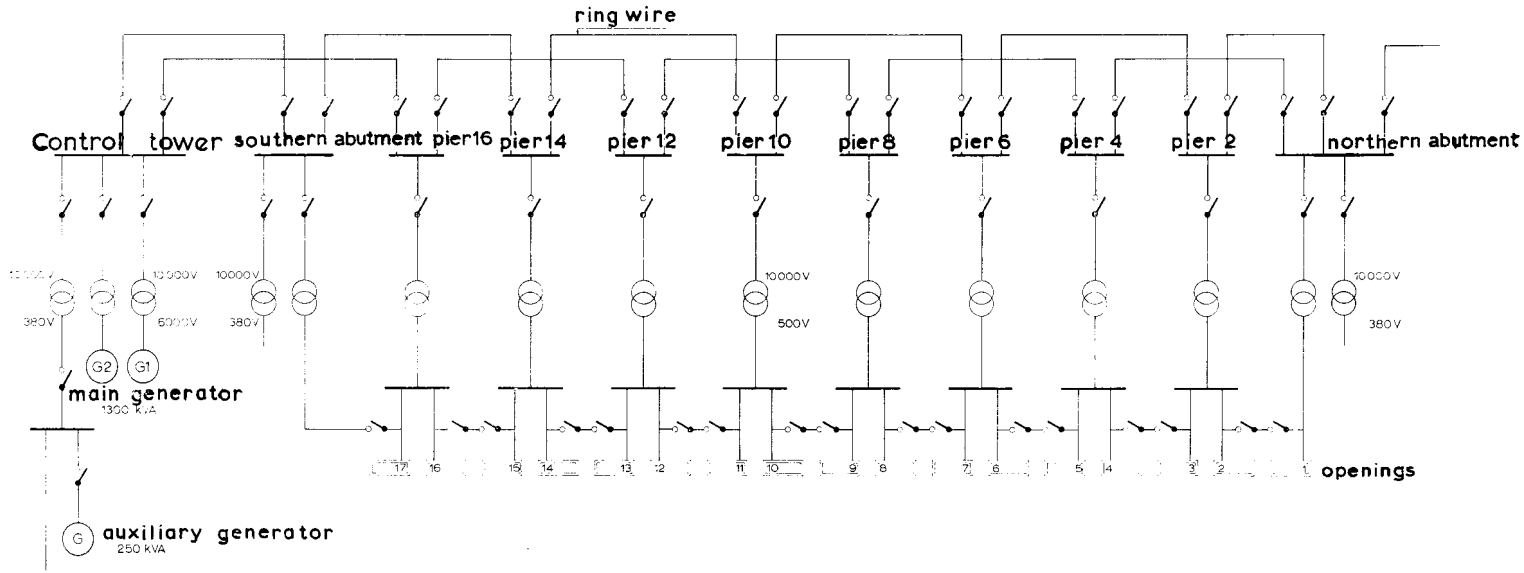

Figure 50. Power supply circuit diagram

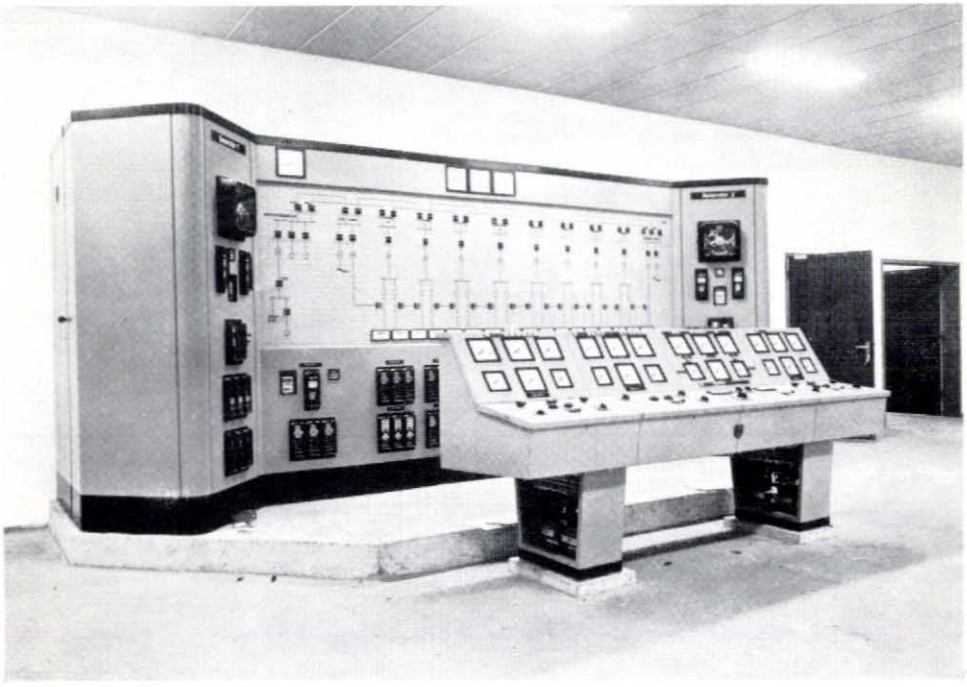

Figure 51. Diesel-electric power plant control panels

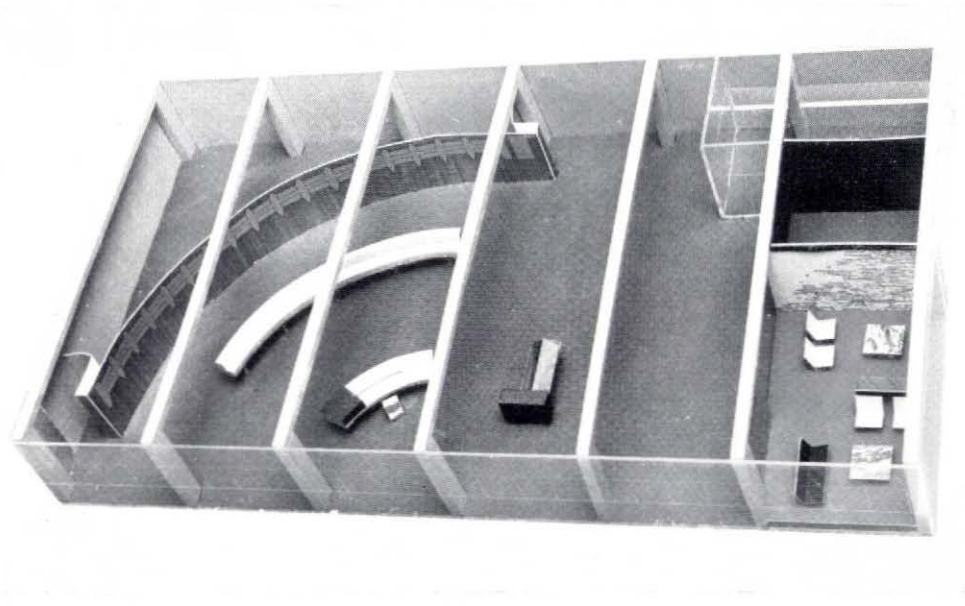

Figure 52. Model of control room

central control room. The panel in the shape of the quadrant of a circle can be seen at the back of the room; all the important signals from the 17 sluice openings with their 34 gates appear on the panel. The height to which each gate is raised is one of the things indicated on it. This is done with selsyns; the sensors are operated by the lifting gear (Figure 43), and transmitted electrically to receivers on the panel.

A telltale on the panel shows when the inflatable rubber sealing tubes have completely sealed off the gaps between gate and pier, and the heating of the concrete pier surfaces on the landward side is also recorded on the panel. The seal surfaces are heated to ensure that the landward gates can be moved in severe frost. The construction of the box-shaped heating elements can be seen in Figure 36: all the compartments are filled with oil which can be heated by means of the electrical resistance wires in them.

The gates are operated from a curved desk in front of the panel. The operator first determines with a selector switch which set of gates he is going to operate, the seaward or the landward ones, after which the required gate opening (in cm) for all the gates is set by means of a counting device and a setting attachment. After thus having prepared the prescribed programme for the entire sluice-gate complex, the operator sets the gates in motion by moving a central switch. The lifting mechanism is automatically switched off when the gates have reached the desired height. The positions of the ends of the gates, which are moved independently, are then adjusted to exactly the same height by the selsyns. Should this sytem be out of commission for some reason or other, the necessary corrections can be made with what are called synchronous switches (Figure 43), which under normal circumstances should move at the same speed for the pair of lifting mechanisms belonging to a single gate. Should they not do so, the faster motor would be switched off as soon as there was a difference between the heights of the two ends of the gate. As a rule, this will return the gate to a horizontal position; the motor switched off is then automatically switched on again. However, in emergencies the difference in lifting height could continue to increase: only in such a contingency would it be necessary to stop both of the lifting mechanisms of the gate concerned.

Spindle switches also operated by the plungers have been fitted; they bring the gates to a stop either in the fully opened or in the fully closed position and operate independently of the safety devices for regulating the position of a gate at both ends.

In conclusion, here are some figures that give some idea of the magnitude of the project:

weight of steel in segmental gates	18,000 tons;
total length of welded seams	350 km;
weight of rolled steel in lifting gear	3,800 tons;
weight of cast steel	4,000 tons;
weight of forged steel	4,500 tons;
length of electric cable conduits	3,300 km.

In the series of Rijkswaterstaat Communications the following numbers have been published before:

Nr 1 *). *Tidal Computations in Shallow Water*
J. J. Dronkers and J. C. Schönfeld
Report on Hydrostatic Levelling across the Westerschelde
A. Waalewijn

Nr 2 *). *Computation of the Decca Pattern for the Netherlands Delta Works*
Ir. H. Ph. van der Schaaf and P. Vetterli, Ing. Dipl. E.T.H.

Nr 3. *The Aging of Asphaltic Bitumen*
Ir. A. J. P. van der Burgh, J. P. Bouwman and G. M. A. Steffelaar

Nr 4. *Mud Distribution and Land Reclamation in the Eastern Wadden Shallows*
Dr. L. F. Kamps †

Nr 5. *Modern Construction of Wing-Gates*
Ir. J. C. le Nobel

Nr 6. *A Structure Plan for the Southern IJsselmeerpolders*
Board of the Zuyder Zee Works

Nr 7. *The Use of Explosives for Clearing Ice*
Ir. J. van der Kley

Nr 8. *The Design and Construction of the Van Brienenoord Bridge across the River Nieuwe Maas*
Ir. W. J. van der Eb †

Nr 9. *Electronic Computation of Water Levels in Rivers during High Discharges*
Section River Studies, Directie Bovenrivieren of Rijkswaterstaat

Nr 10. *The Canalization of the Lower Rhine*
Ir. A. C. de Gaay and Ir. P. Blokland

*) out of print